

# **Tornadoes in Nonmesocyclone Environments with Pre-existing Vertical Vorticity along Convergence Boundaries**

James M. Caruso  
National Weather Service, Wichita, Kansas

Jonathan M. Davies  
Private Meteorologist, Wichita, Kansas

Published in the NWA *Electronic Journal of Operational Meteorology* 1 June  
2005  
(updated 12 December 2005)

---

## **1. Introduction**

Tornadoes resulting from stretching of pre-existing vertical vorticity along convergence boundaries are not unusual in the warm season in the central plains of the United States. These tornadoes are associated mainly with nonmesocyclone processes (Brady and Szoke 1989), sometimes called "nonsupercell" (Wakimoto and Wilson 1989), with the tornadoes often called "landspouts" (Bluestein 1985). In some cases, tornadoes in such environments can reach significant intensity (defined here as F2 or greater on the Fujita scale), particularly if instability is large. One example is the nonmesocyclone tornadoes that hit the Denver, Colorado area on 15 June 1988 (Wakimoto and Wilson 1989); two of the four tornadoes caused F2 and F3 damage. Another example is a case examined in this study with an F2 intensity nonmesocyclone tornado near Wellington, Kansas on 27 August 2004 that lasted nearly 20 minutes. So, it seems clear that some nonmesocyclone tornadoes can present a significant threat to property and lives, suggesting that terminology such as "landspout" (interpreted by many to mean "weak tornado") may at times be misleading or inappropriate. Nonmesocyclone tornadoes are typically more difficult to anticipate and forecast than supercell/mesocyclone tornadoes, which have been more widely researched.

This paper will review a common mesoscale setting that appears to be favorable for nonmesocyclone tornadoes resulting from pre-existing vertical circulations

along wind shift boundaries. Discussion and examples will also focus on low-level thermodynamic characteristics that appear to be associated with such tornadoes and their environments, as well as radar identification of boundaries that play a role in such events. Three cases involving nonmesocyclone tornadoes during 2002-2004 in south central Kansas will serve as events for examination. It is hoped that this study will increase situational awareness for mesoanalysts and warning meteorologists regarding some nonmesocyclone tornado environments.

## **2. Nonmesocyclone tornado environments**

A common surface setting associated with nonmesocyclone tornadoes identified informally by Davies (2003) involves a slow-moving or stationary wind shift boundary (typically a weak front or trough without a strong temperature contrast), often oriented northeast to southwest (Fig. 1). Winds shifting from southerly to westerly or northwesterly across the boundary generate convergence and potential for pre-existing vertical vorticity circulations (Brady and Szoke 1989; Wakimoto and Wilson 1989) or mesocyclones (Fujita 1981). Smaller scale thunderstorm outflow boundaries or horizontal convective rolls intersecting the boundary can also provide focus for vertical vorticity circulations.

An important thermodynamic feature of this setting is a surface heat axis that parallels or intersects the main wind shift boundary, generating an area of steep low-level lapse rates within the lowest 2 or 3 km above ground. In tornadic cases, this axis of steep low-level lapse rates will typically overlap an area of low-level CAPE (e.g., 0-3 km CAPE, Rasmussen 2003) somewhere along the boundary. The presence of CAPE below 3 km suggests small convective inhibition (CIN), and sufficient quality and depth of moisture to maintain significant buoyancy for mixed-layer lifted parcels, indicating that thunderstorm updrafts along the boundary will be significantly surface-based. When combined with steep low-level lapse rates, these thermodynamic characteristics (in addition to significant total CAPE for deep convection) suggest potential for rapid low-level accelerations beneath updrafts, resulting in enhanced vertical stretching with little or no resistance to rising parcels. In such environments, nonmesocyclone tornadoes can occur when a vigorous developing updraft is juxtaposed with a pre-existing vertical vorticity circulation along the main wind shift boundary. Tornado development results from the vertical stretching of these circulations, enhanced by the low-level thermodynamic environment.

This process is shown in [Fig. 2](#), reproduced from Wakimoto and Wilson (1989). Nonmesocyclone tornadoes typically develop early in a storm's life-cycle (e.g., Burgess et al. 1993) during the updraft stage, whereas mesocyclone tornadoes occur during a supercell storm's mature stage when significant downdrafts have organized around the main updraft (e.g., Lemon and Doswell 1979). Because nonmesocyclone tornadoes can develop early and rapidly, mesoanalysis of pre-existing surface features where thunderstorm development is expected is crucial to anticipate them. Parameters such as large storm-relative helicity (SRH, Davies-Jones et al. 1990) and low lifting condensation levels (LCL heights, e.g., Rasmussen and Blanchard 1998) used in forecasting supercell/mesocyclone tornadoes are generally not relevant to nonmesocyclone tornadoes because the formation processes are different. Slow boundary-relative storm motion is typical with nonmesocyclone tornadoes, and as noted by Davies (2003), the southernmost cells on radar are often most favored for tornadoes. Settings similar to [Fig. 1](#) can often support events lasting up to an hour or more, involving multiple nonmesocyclone tornadoes.

The following sections will examine three recent cases of tornadoes developing in nonmesocyclone environments over south central Kansas. These cases will highlight the importance of mesoscale boundaries and low-level thermodynamic characteristics. Thermodynamic variables such as total CAPE and 0-3 km CAPE in this study were computed using lowest 100 mb mixed-layer lifted parcels (denoted as "ML"; e.g., MLCAPe) similar to Thompson et al. (2003). The virtual temperature correction (Doswell and Rasmussen 1994) was used in thermodynamic computations.

### **3. 27 August 2004 case**

Four tornadoes associated with a nonmesocyclone environment occurred in south central Kansas on 27 August 2004 between 0000 UTC and 0100 UTC. The strongest tornado was rated F2, and touched down about 3 km (2 mi) south of Wellington, Kansas ([Fig. 3](#)), causing \$250,000 damage with a maximum path width of roughly 100 m (110 yds) and a path length of 5 km (3 mi). This tornado lasted nearly 20 minutes and had a large, full condensation funnel extending all the way to the ground from a high cloud base, not the typical visual appearance of a so-called "landspout".

The synoptic setting involved an upper level shortwave trough (not shown)

located upstream in Colorado, with the tornadoes occurring in an environment of weak deep-layer shear, well to the southeast of the shortwave feature and stronger winds aloft. On the mesoscale, the surface map at 2300 UTC (Fig. 4) showed a weak quasi-stationary front oriented northeast to southwest across south central Kansas and a weak low over north central Oklahoma. The atmosphere was extremely unstable with MLCAPE of 3500 to 4000 J kg<sup>-1</sup> (Fig. 5) across south central Kansas. A Rapid Update Cycle (RUC, Benjamin et al. 2004) model analysis sounding, similar to those used in Thompson et al. (2003) and Davies (2004), is shown in Fig. 6 at 2300 UTC for Winfield, Kansas, 40 km east of the location where the F2 tornado occurred 90 min later. This profile indicated that steep 0-2 km lapse rates (near 9.0 °C km<sup>-1</sup>) were present, along with deep low-level moisture, resulting in substantial 0-3 km MLCAPE (around 90 J kg<sup>-1</sup>) and very little convective inhibition (MLCIN). The environment was not suggestive of supercell tornadoes, with only small 0-1 km SRH (< 50 m<sup>2</sup>s<sup>-2</sup>) and high MLLCL heights (> 1600 m AGL).

Figure 7 shows parameter fields of 0-2 km lapse rate and 0-3 km MLCAPE generated from the RUC model at 2300 UTC on 27 August 2004. Notice that steep low-level lapse rates and low-level CAPE were juxtaposed in an area over south central Kansas and north central Oklahoma, along the quasi-stationary front where thunderstorms were developing. As discussed in the prior section, this low-level thermodynamic setting suggested some potential for rapid parcel ascent and enhanced low-level stretching. The mesoscale and thermodynamic setting matched the composite pattern in Fig. 1 rather well.

A visible satellite image at 2303 UTC (Fig. 8) showed rapidly developing thunderstorms across south central Kansas in a narrow northeast to southwest axis along the frontal zone. An outflow boundary that intersected the main frontal zone at a break in this line of storms can be seen in the radar reflectivity image in Fig. 9a, forming a "triple-point" (Lemon and Quetone 1995, and others). This boundary intersection likely served to increase low-level convergence and pre-existing vertical vorticity on the front northeast of the weak surface low. Figure 9b is a radar reflectivity loop showing the back-building nature of the multicell storms over south central Kansas and the evolution of the boundary intersection. A 4-panel display of base reflectivity from the KICT WSR-88D radar at 0046 UTC 28 August 2004 (Fig. 10) shows the rapid updraft development (5.1 degree

slice) that occurred over the low-level boundary intersection convergence zone (0.5 degree slice). The F2 tornado was in progress at this time south of Wellington.

Figure 11 shows the base velocity for the same time and slices as in Fig. 10. Base velocity was in use instead of velocity from storm-relative motion (SRM) because of very slow storm movement. A tight couplet with maximum rotational velocity of 41 kt located at elevation angles 1.8 through 10.0 degrees (5,461 - 29,000 ft AGL) is seen in Fig. 11, coinciding with the rapid updraft development over the low-level boundary intersection convergence zone. The base velocity data also indicated that the rotation began in the lower levels of the storm and built upward into middle levels between 0029 UTC and 0046 UTC. Radar data provided no evidence of a pre-existing midlevel mesocyclone or supercell structure prior to the tornado that occurred from 0030 UTC to 0049 UTC. There were no indications of a weak echo region (WER), bounded weak echo region (BWER), inflow notch, rear-flank downdraft (RFD), or hook echo before the tornado was on the ground. This raises the following question: Was the velocity couplet in Fig. 11 a rapidly developing supercell mesocyclone, or simply the radar sampling the increasing circulation around the tornado? Most important, from an operational perspective, this velocity couplet was not evident before the tornado occurred, yet the low-level boundary intersection and evolution was quite visible in radar imagery well in advance of the tornado.

Developing and maintaining situational awareness regarding mesoscale features and thermodynamic environments that may have potential for nonmesocyclone tornadoes can help forecasters react quickly in issuing tornado warnings as radar features evolve, as described above. Although it is difficult for WSR-88D radar to detect low-level precursors (boundaries or pre-existing low-level circulations) beyond ranges of roughly 80 km (45 nm) due to problems with the radar horizon and beam width spreading (Warning Decision Training Branch 2002), this case fortunately occurred relatively close to the radar site. Even with no prior mesocyclone on radar, the boundary intersection and low-level thermodynamic setting were features that could be noted and assessed in advance of the tornado.

#### **4. 9 July 2003 case**

During the late afternoon and evening on 9 July 2003, severe thunderstorms developed along a frontal boundary oriented northeast-southwest in central Kansas

(Fig. 12). Severe weather reports included eight tornadoes, several severe wind gusts (50 kt or greater), and large hail ranging from 4.5 cm (golfball size) to 11 cm (softball size). The strongest tornado, rated F1, occurred about 8 km (5 mi) southeast of Cunningham, Kansas, and had a path length of 8 km (5 mi) with a path width of roughly 90 m (100 yards).

A surface heat axis at late afternoon (not shown) paralleled the weak frontal zone, intersecting it over south central Kansas. Similar to the prior case, the atmosphere was quite unstable with MLCAPE of 2500 to 3500 J kg<sup>-1</sup> (not shown) across south central Kansas. A RUC analysis sounding (Fig. 13) at 2300 UTC at Kingman, Kansas, located 27 km east-northeast of the location where the F1 tornado occurred 90 min later, suggested several characteristics relevant to nonmesocyclone tornado potential. These included very steep low-level lapse rates (near 10.0 °C km<sup>-1</sup>) along with a deep low-level moist layer that resulted in 0-3 km MLCAPE (around 40 J kg<sup>-1</sup>) and negligible MLCIN, even though MLLCL heights were quite high (> 2000 m AGL). In addition, significant 0-6 km shear (38 kt) and 0-1 km SRH (near 100 m<sup>2</sup>s<sup>-2</sup>, larger than in the prior case) suggested that the environment was also marginally favorable for supercell tornadoes, making for a more complicated environment setting. The RUC analysis fields in Fig. 14 show that low-level lapse rates and low-level CAPE overlapped significantly in south central Kansas at 0000 UTC 10 July 2003, suggesting potential for rapid parcel ascent and enhanced low-level stretching with updrafts along the frontal boundary. Thunderstorms were in progress along this boundary at 0000 UTC, back-building to the south-southwest, with several tornadoes occurring between 0000 UTC and 0100 UTC (Fig. 14).

Reflectivity and velocity images in Fig. 15a show the intersection of the northeast-southwest front with a thunderstorm outflow boundary across western Kingman County at 0034 UTC 10 July 2003 at the time the F1 tornado noted earlier was occurring. In the reflectivity, a large thunderstorm can be seen extending to the immediate east-northeast of the boundary intersection. The thunderstorm exhibited some supercell characteristics as it moved slowly southward across Reno, Kingman, and Harper Counties during the late afternoon and early evening hours, producing very large hail. As the thunderstorm pushed southward, its outflow boundary moved southwestward, persistently intersecting the main frontal zone (see radar reflectivity loop in Fig. 15b). The boundary intersection area (a source of pre-existing vorticity) appeared to stay within the flanking line structure of the supercell, and radar imagery suggested that a series of strong updrafts

developed over this boundary intersection area in repetitive fashion, with resulting tornadoes. At the time of the F1 tornado southeast of Cunningham, the SRM velocity data in Fig. 15a showed two low-level velocity couplets near the tornado location. However, radar evidence of a pre-existing midlevel mesocyclone was located several kilometers to the northeast of the reported tornado.

This case is an excellent example of how nonmesocyclone tornadoes can occur in conjunction with a supercell thunderstorm. It also demonstrates a potential problem where a radar operator, who might be unaware of the possibility of nonmesocyclone tornadoes, could be focused on the "wrong" part of the storm (the midlevel mesocyclone). This would make it more difficult to understand or accept observed reports of funnel clouds or tornadoes farther to the southwest. Also, a forecaster thinking more in terms of supercell/mesocyclone tornado settings and unaware of the potential for nonmesocyclone tornadoes might be confused and surprised when tornado reports began to materialize in an environment with relatively high cloud bases and LCL heights (e.g., Rasmussen and Blanchard 1998).

## **5. 11 April 2002 case**

Two tornadoes, both rated F0, occurred near peak heating during the late afternoon of 11 April 2002 in south central Kansas between 2200 and 2300 UTC in a nonmesocyclone environment. Figure 16 shows one of the tornadoes southeast of Pretty Prairie, Kansas, lasting between 15 and 20 minutes, emanating from a high, flat cloud base.

The surface map at 2300 UTC (Fig. 17) showed a weak quasi-stationary frontal boundary oriented northeast to southwest across central Kansas, with a surface heat axis (not shown) paralleling and intersecting the front in south central Kansas. The atmosphere was less unstable than in the prior cases, but still moderately unstable with MLCAPE of 1000 to 1500 J kg<sup>-1</sup> indicated by ETA analysis fields at 2100 UTC (Fig. 18) in an environment with weak deep-layer shear (< 30 kt, not shown). A RUC analysis sounding (Fig. 19) at 2200 UTC for Hutchinson, Kansas (located about 40 km north-northeast of the Pretty Prairie tornado) suggested several nonmesocyclone tornado environment characteristics. Very steep low-level lapse rates (9.5 to 10.0 °C km<sup>-1</sup>) were present along with deep low-level moisture that resulted in small MLCIN and notable 0-3 km MLCAPE (around 40 J kg<sup>-1</sup>), even though MLLCL heights were above 1500 m

AGL. The sounding also indicated that 0-1 km SRH was small ( $< 25 \text{ m}^2\text{s}^{-2}$ ), suggesting an unfavorable environment for supercell tornadoes. But combinations of steep low-level lapse rates and substantial 0-3 km MLCAPE (Fig. 20) were maximized along the frontal boundary in south central Kansas where the tornadoes occurred, suggesting increased potential for low-level stretching with updrafts along the boundary. Like the prior cases, this case also closely matched the composite pattern for nonmesocyclone tornadoes in Fig. 1.

Figure 21a is the KICT 0.5 degree base reflectivity image at 2234 UTC when thunderstorms were in progress along the northeast-southwest frontal zone. The yellow arrows in Fig. 21a indicate the direction of the low-level wind at specific locations, and the white ellipses highlight likely areas of pre-existing vertical vorticity. Note that the lower left ellipse indicates a wavelike inflection signature along the front (e.g., Pietrycha and Manross 2003), and the top two ellipses show the intersections of thunderstorm outflow boundaries with the front. The tornado in Fig. 16 was in progress at the time of Fig. 21a, at the location where the purple arrow points to a new updraft developing over one of these intersections. The back-building nature of the thunderstorms and evolution of the frontal/outflow boundary intersections can be seen in the radar reflectivity loop in Figure 21b. SRM velocity data during and prior to the tornado (not shown) did not indicate significant rotations, nor did it show any evidence of a pre-existing midlevel mesocyclone. As with the prior cases, data suggests that the low-level boundary intersection (a source of vertical vorticity), and the thermodynamic environment (favorable for rapid low-level stretching), were important factors supporting development of nonmesocyclone tornadoes in this case.

## 6. Conclusion

All three of the tornado events in this study fit a composite pattern supportive of nonmesocyclone tornadoes identified by Davies (2003) as shown in Fig. 1. A weak, slow-moving or stationary surface front with little temperature contrast, but a sharp wind shift from south or southwest to northwest winds was evident in all cases examined. The frontal wind shift boundary was oriented northeast to southwest, and was important in providing low-level convergence and pre-existing low-level vertical vorticity. Along this wind shift boundary, very steep low-level lapse rates were found to overlap substantial low-level CAPE and total CAPE, likely enhancing low-level stretching of parcels entering storm updrafts on the

boundary. In all cases examined, nonmesocyclone tornadoes occurred where new strong updrafts developed over the intersection of a thunderstorm outflow boundary with the main frontal zone, similar to the case presented in Lemon and Quetone (1995). Tornadogenesis appeared to occur early in the updraft life cycles when low-level stretching occurred at the frontal/outflow boundary intersections, enhanced by the low-level thermodynamic environment. This is in contrast to supercell/mesocyclone tornadoes, which normally occur during a supercell storm's mature stage when downdrafts (e.g., the rear flank downdraft) are well organized. Atmospheric instability varied from moderate to extreme in the three cases studied.

Two of the three tornado cases examined (27 August 2004 and 11 April 2002) had environments with small SRH and weak deep-layer shear. This is in contrast to supercell tornado environments where SRH is typically large, deep-layer shear is strong, and LCL heights are low. The remaining tornado case (9 July 2003) appeared to be a "hybrid" setting, fitting the composite pattern and thermodynamic characteristics from Davies (2003), but also exhibiting SRH and 0-6 km shear values that were marginally favorable for supercells. The result was nonmesocyclone tornadoes associated with a high-based supercell thunderstorm. The tornadoes appeared to occur within the storm's flanking line instead of with the midlevel mesocyclone.

As noted earlier, nonmesocyclone tornado environments can support events lasting up to an hour or more, involving multiple tornadoes. Two of the tornadoes documented in this study lasted nearly 20 minutes in duration, with one causing significant (F2) damage. This emphasizes that some nonmesocyclone tornadoes can present a significant threat to life and property. Because nonmesocyclone tornadoes are not preceded by midlevel or low-level mesocyclones, WSR-88D velocity data is usually of limited use in the traditional mode of tornado warning by radar for most tornadoes in nonmesocyclone environments. However, at closer ranges (e.g., within 60-80 km of the radar), velocity and reflectivity data from the WSR-88D can be useful for identifying and tracking storm-scale/mesoscale boundaries to suggest areas of enhanced pre-existing vorticity (see [Figs. 9a](#), [15a](#), and [21a](#)). As seen in Pietrycha and Manross (2003), low-level circulations along slow-moving frontal boundaries or troughs are often discernible in velocity and reflectivity products when not too far from the radar site.

Identification of such features, as well as recognition of the setting and common

ingredients supportive of nonmesocyclone tornadoes (e.g., [Fig. 1](#)) can provide heightened short-term awareness to forecasters and warning meteorologists. Such knowledge may offer lead time for deploying storm spotters to areas of greatest concern, helping to anticipate tornado reports that might otherwise be a “surprise” without appropriate situational awareness. It may also be possible to issue more rapid tornado warnings when a combination of environment awareness, spotters, and radar are used together (e.g., Cook et al. 2005).

Mesoanalysis is crucial for recognizing in advance the thermodynamic ingredients and boundaries that can be conducive to nonmesocyclone tornadoes. Prior to thunderstorm formation, environments with potential for nonmesocyclone tornadoes can be diagnosed using careful surface mesoanalysis, satellite imagery, soundings (such as from Local Analysis and Prediction System (LAPS) and RUC model data), and radar imagery (e.g., Pietrycha and Manross 2003, and Cook et al. 2005). Radar data, particularly high resolution 8 bit base reflectivity and velocity products within 60 km range and overlain with surface data (such as METAR plots), can be very useful for finding boundaries and boundary intersections to suggest areas of enhanced pre-existing vertical vorticity. Results from this study also suggest that assessing combinations of steep low-level lapse rates and positive low-level CAPE in the vicinity of mesoscale wind shift boundaries through examination of the overlapping fields may be helpful in assessing nonmesocyclone tornado potential. It is important to remember that most nonmesocyclone tornadoes occur in environments characterized by small SRH and high LCL heights, contrasting with more "typical" supercell tornado environments that are emphasized in forecaster training.

Further research is planned regarding application of the concepts and parameters reviewed in this paper to future nonmesocyclone tornado events.

### ***Acknowledgments:***

The authors would like to thank Ken Cook and Paul Howerton, both at NWS Wichita, for their review and comments on this paper. Thanks is also extended to Dan Baumgardt at NWS La Crosse for incorporating several experimental nonmesocyclone environment parameters, pertaining to research by Davies (2003), into the AWIPS Volume Browser. Sincere thanks also go to [Jim Reed Photography](#) and John Brand for their tornado images used in this paper.

## References:

Benjamin, S. G., D. Devenyi, S. S. Weygandt, K. J. Brundage, J. M. Brown, G. A. Grell, D. Kim, B. E. Schwartz, T. G. Smirnova, T. L. Smith, and G. S. Manikin, 2004: An hourly assimilation-forecast cycle: The RUC. *Mon. Wea. Rev.*, **132**, 495-518.

Bluestein, H. B., 1985: The formation of a “landspout” in a “broken-line” squall line in Oklahoma. Preprints, *14<sup>th</sup> Conf. on Severe Local Storms*, Indianapolis, IN, Amer. Meteor. Soc., 267-270.

Brady, R.H., and E.J. Szoke, 1989: A case study of nonmesocyclone tornado development in northeast Colorado: similarities to waterspout formation. *Mon. Wea. Rev.*, **117**, 843-856.

Burgess, D. W., R. J. Donaldson Jr., and P. R. Desrochers, 1993: Tornado detection and warning by radar. *The Tornado: Its Structure, Dynamics, Prediction, and Hazards, Geophys. Monogr.*, No. 79, Amer. Geophys. Union, 203-221.

Cook, K. R., D. Baumgardt, and T. Shea, 2005: Increasing situational awareness for nonsupercell tornadogenesis: 16 June 2004. *9<sup>th</sup> Annual Northern Plains Convective Workshop*, St. Paul, MN, March 2005. Available on the workshop CD.

Davies, J. M., 2003: Ingredients supporting nonmesocyclone tornado events. Available on the web at:  
[http://members.cox.net/jondavies1/tornado\\_fcsting/nonsprcell\\_tors.htm](http://members.cox.net/jondavies1/tornado_fcsting/nonsprcell_tors.htm)

-----, 2004: Estimations of CIN and LFC associated with tornadic and nontornadic supercells. *Wea. Forecasting*, **19**, 714-726.

Davies-Jones, R. P., D. Burgess, and M. Foster, 1990: Test of helicity as a tornado forecast parameter. Preprints, *16<sup>th</sup> Conf. on Severe Local Storms*, Kananaskis Park, AB, Canada, Amer. Meteor. Soc., 588-592.

Doswell, C. A. III, and E. N. Rasmussen, 1994: The effect of neglecting the virtual temperature correction on CAPE calculations. *Wea. Forecasting*, **9**, 625-629.

Fujita, T.T., 1981: Tornadoes and downbursts in the context of generalized planetary scales. *J. Atmos. Sci.*, **38**, 1511-1534.

Lemon, L. R., and E. M. Quetone, 1995: WSR-88D and visual observations of a non-supercellular storm and tornado. Preprints, *27<sup>th</sup> Conf. on Radar Meteorology*, Vail, CO, Amer. Meteor. Soc., 156-159.

-----, and C. A. Doswell III, 1979: Severe thunderstorm evolution and mesocyclone structure as related to tornadogenesis, *Mon. Wea. Rev.*, **107**, 1184-1197.

Pietrycha, A. E., and K. L. Manross, 2003: WSR-88D analysis of vorticies embedded within a surface low pressure trough and subsequent convection initiation. Preprints, *31st Int. Conf. on Radar Meteorology*, Seattle, WA, Amer. Meteor. Soc., 835-838.

Rasmussen, E. N., 2003: Refined supercell and tornado forecast parameters. *Wea. Forecasting*, **18**, 530-535.

-----, and D. O. Blanchard, 1998: A baseline climatology of sounding-derived supercell and tornado forecast parameters. *Wea. Forecasting*, **13**, 1148-1164.

Thompson, R. L., R. Edwards, J. A. Hart, K.L. Elmore, and P. Markowski, 2003: Close proximity soundings within supercell environments obtained from the Rapid Update Cycle. *Wea. Forecasting*, **18**, 1243-1261.

Wakimoto, R. M., and J. W. Wilson, 1989: Non-supercell tornadoes. *Mon. Wea. Rev.*, **117**, 1113-1140.

Warning Decision Training Branch, 2002: Tornado Warning Guidance Document - 2002 Version. Available on the web at: <http://www.wdtb.noaa.gov/modules/twg02/TWG2002.pdf>

A typical setting that may support non-mesocyclone tornadoes (example from April 2002)

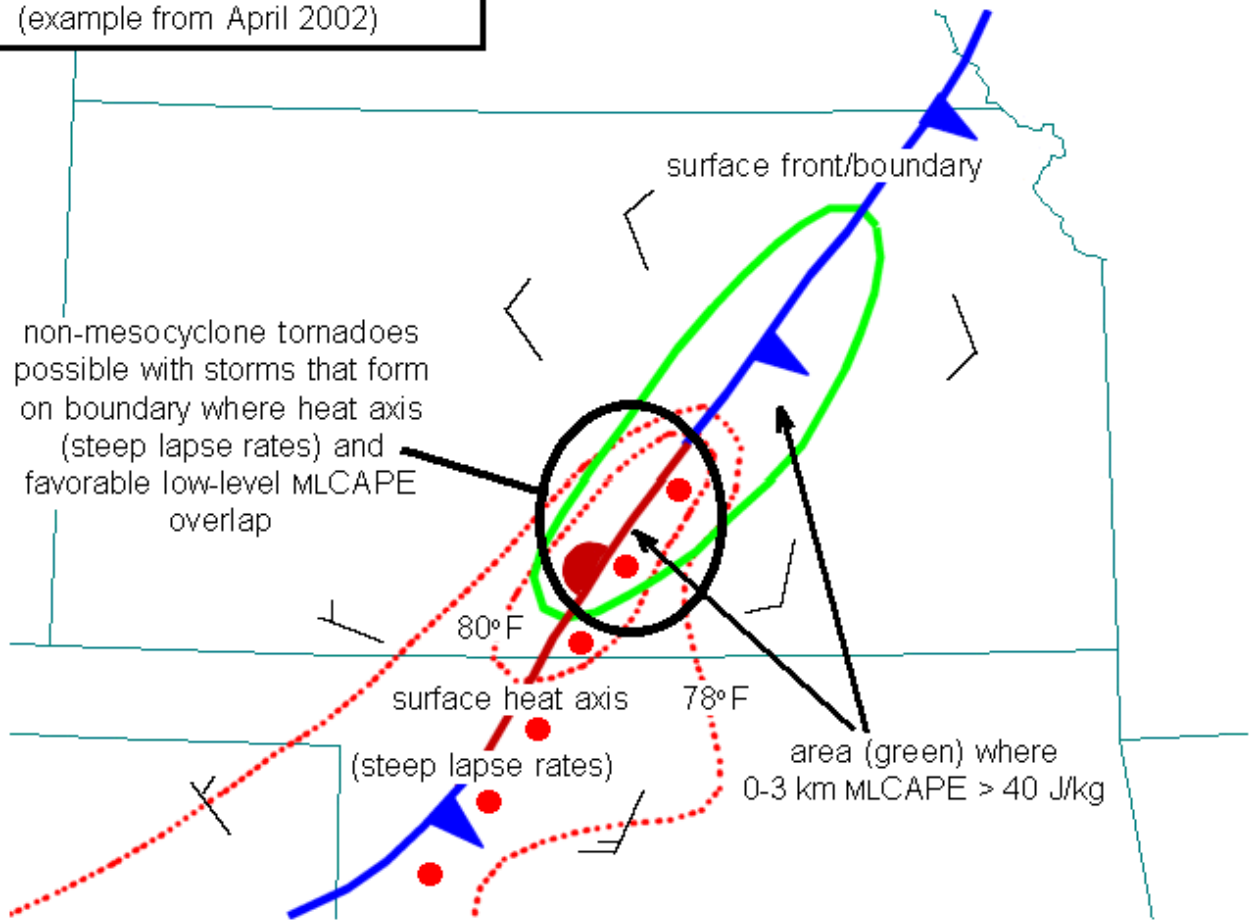


**Figure 1:** Composite example by Davies (2003) depicting a typical setting that can support nonmesocyclone tornadoes. Important features are labeled; red dots denote surface heating axis of steep lapse rates; area enclosed in green denotes 0-3 km MLCAPE > 40 J kg<sup>-1</sup>; wind flags show surface flow ahead of and behind frontal boundary.

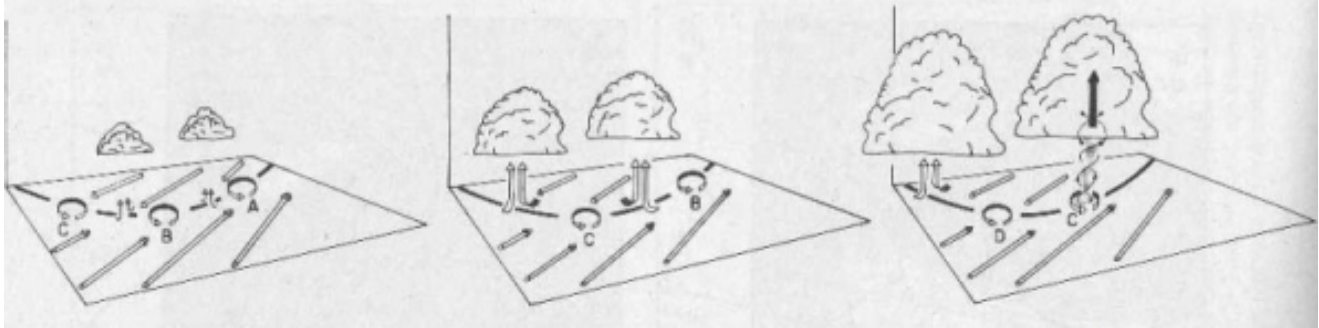


**Figure 2:** Schematic model of the life cycle of a nonmesocyclone tornado. The black line is the wind shift convergence boundary; horizontal arrows indicate surface wind flow; vertical arrows indicate updrafts. Low-level vortices are labeled with letters (from Wakimoto and Wilson 1989).

Courtesy John Brand



**Figure 3:** Nonmesocyclone tornado rated F2 in intensity south of Wellington, Kansas on 27 August 2004 (photo courtesy John Brand).

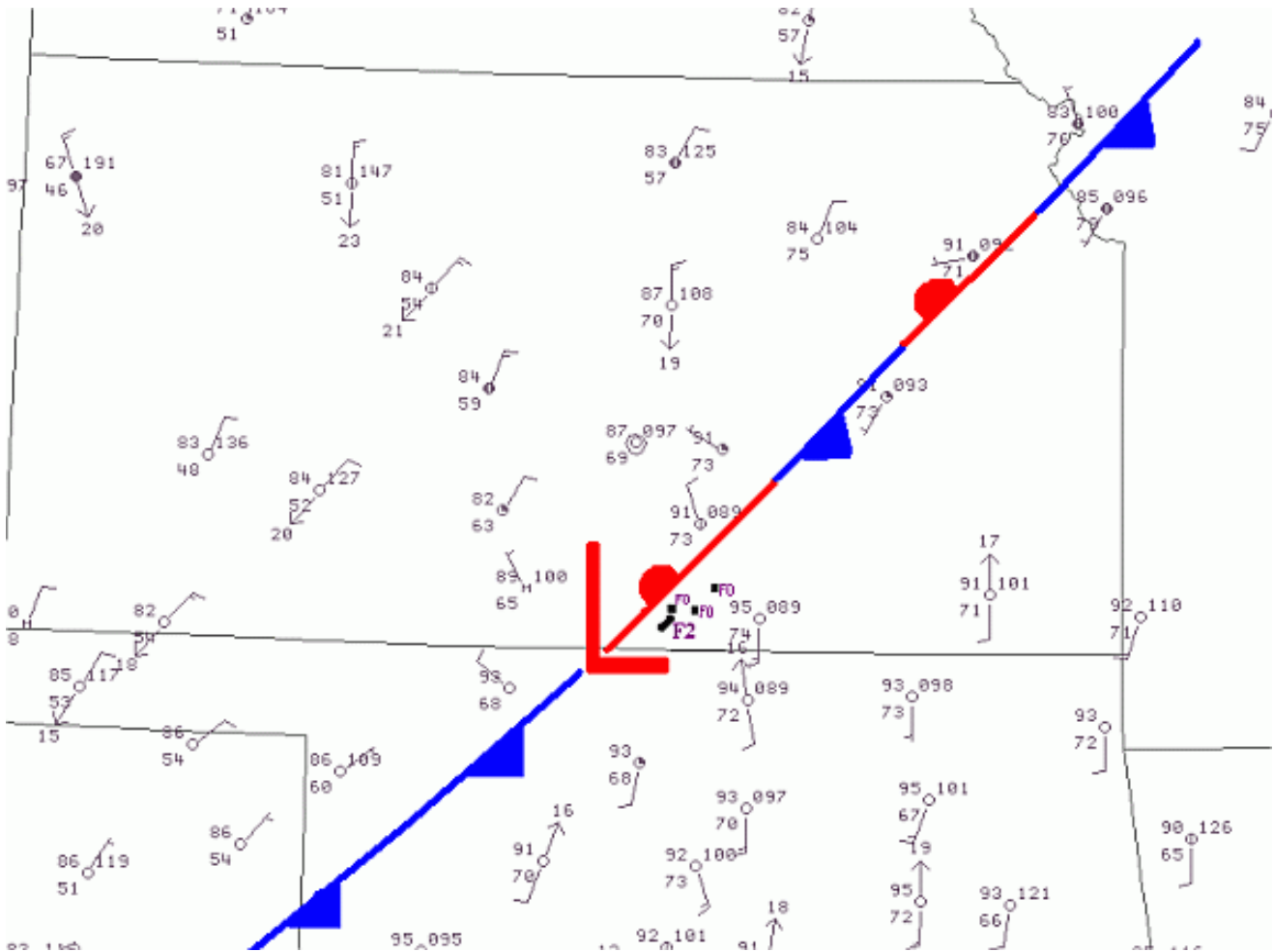


**Figure 4:** Surface map at 2300 UTC 27 August 2004 with frontal boundary and mesocyclone indicated. Tornado path locations and F-scales 0000 UTC to 0100 UTC 28 August 2004 are also shown.

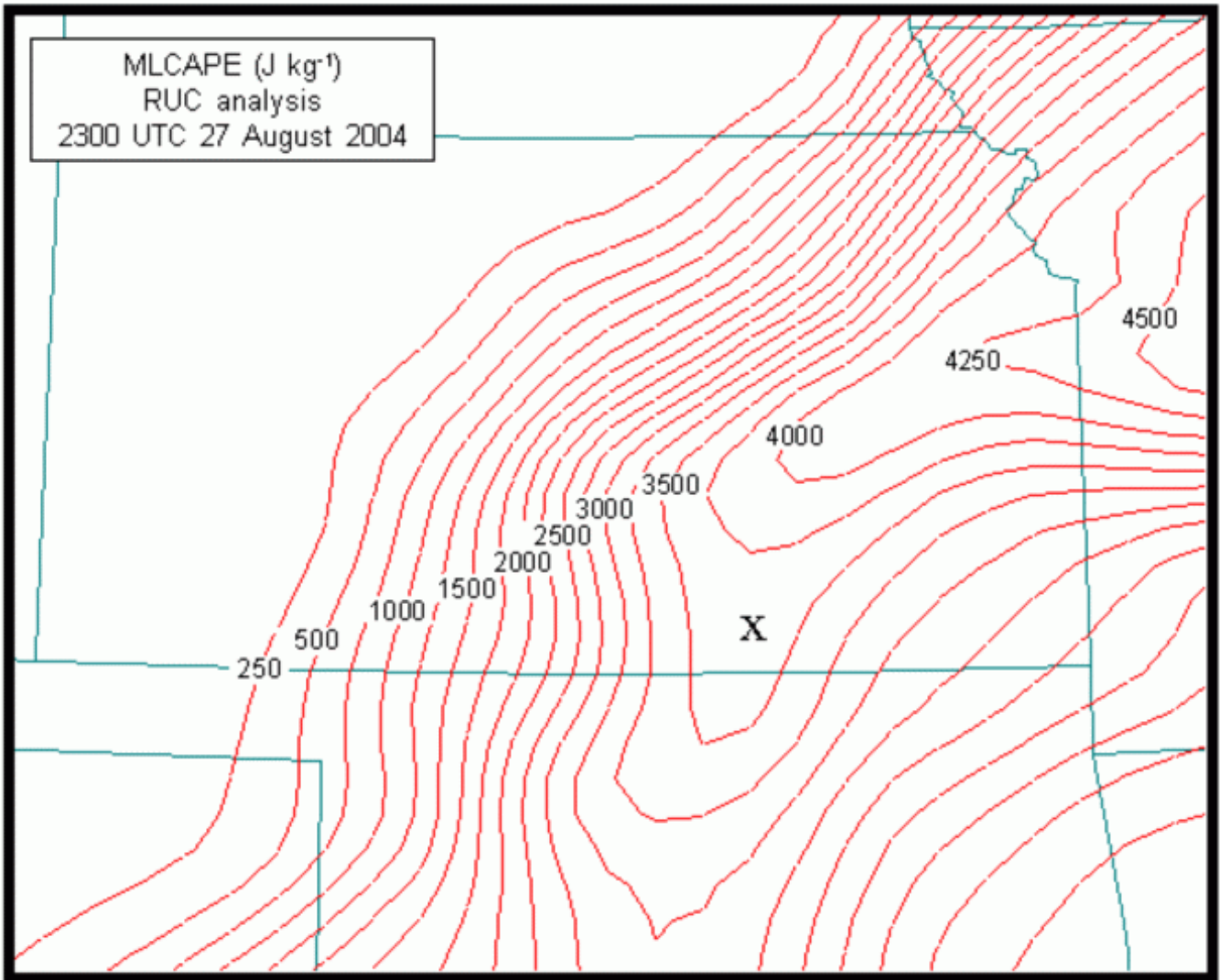


**Figure 5:** Estimated field of MLCAPE ( $\text{J kg}^{-1}$ ) computed from RUC analysis at 2300 UTC 27 August 2004. The letter "X" denotes the location of the RUC model analysis sounding shown in [Fig. 6](#).

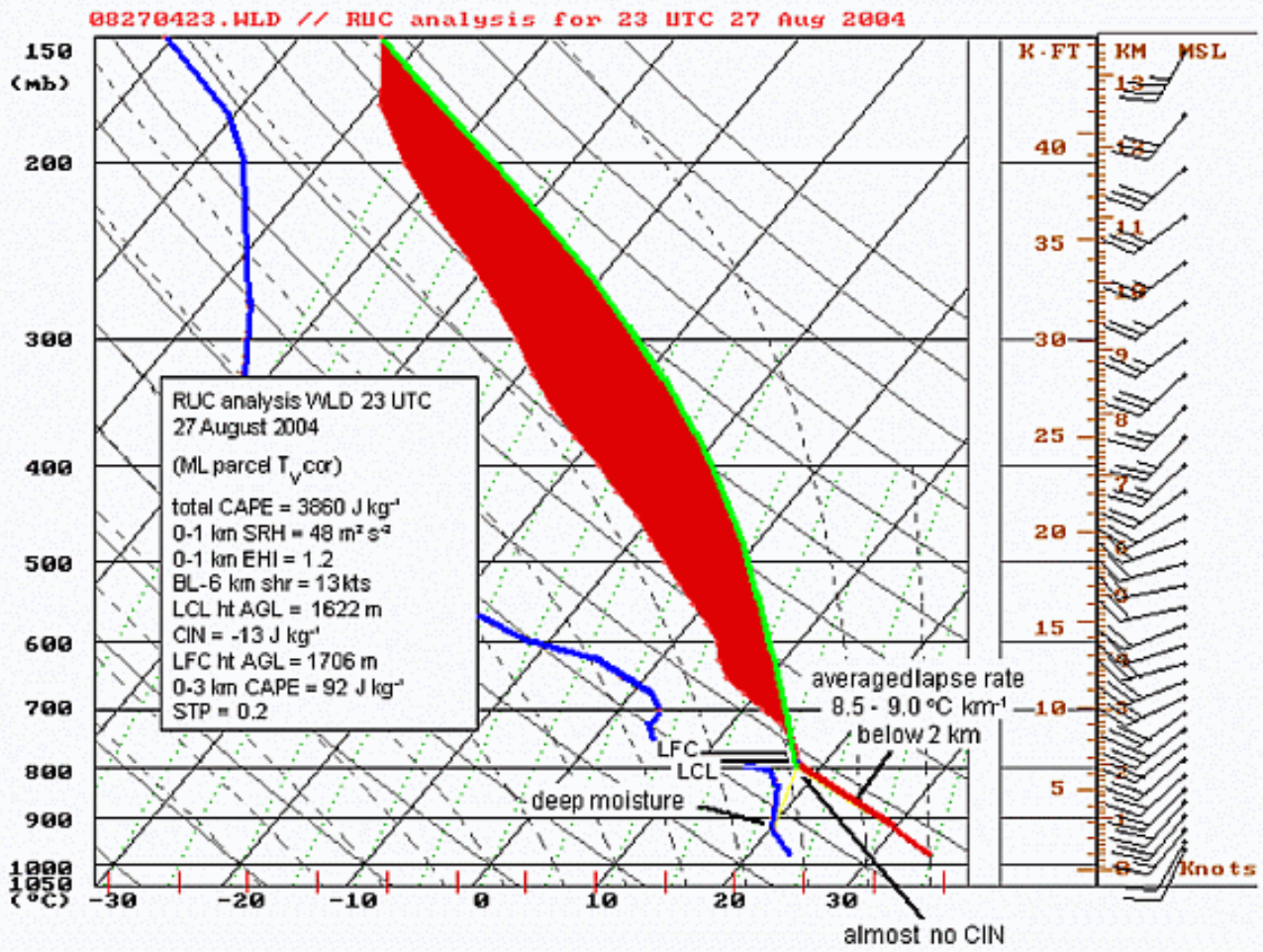


**Figure 6:** SkewT-logp diagram of RUC analysis sounding for Winfield, Kansas at 2300 UTC 27 August 2004, location shown in Fig. 5. Important features are labeled.

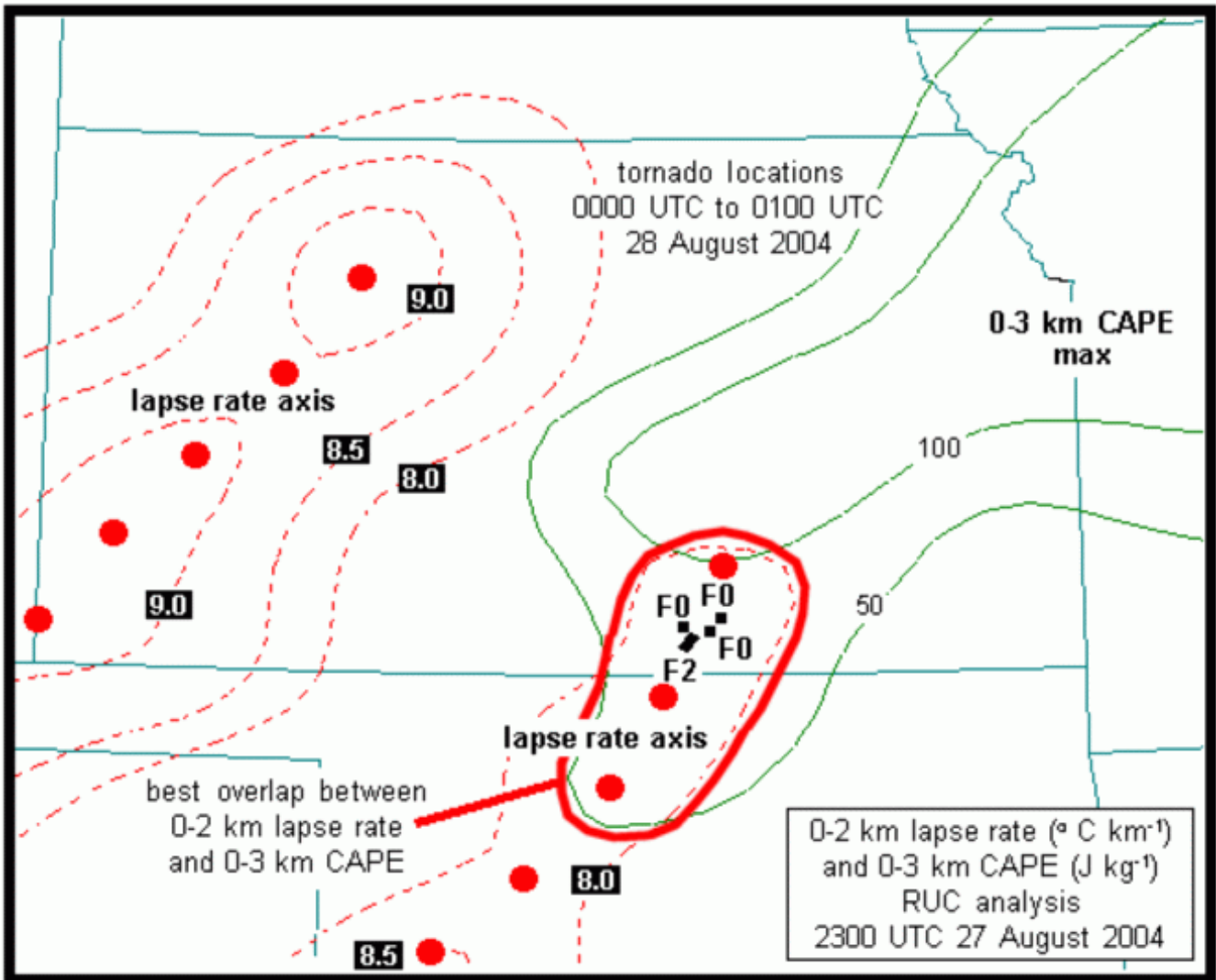


**Figure 7:** As in Fig. 5, except for 0-2 km lapse rate ( $\geq 8^{\circ}\text{C km}^{-1}$ , dashed red lines) and 0-3 km CAPE ( $\geq 50\text{ J kg}^{-1}$ , solid green lines) at 2300 UTC 27 August 2004. Area of best overlap between these two fields is enclosed in heavy solid red. Heavy red dots denote axes of steepest low-level lapse rates. Tornado path locations 0000 UTC to 0100 UTC 28 August 2004 are shown in black with F-scales.

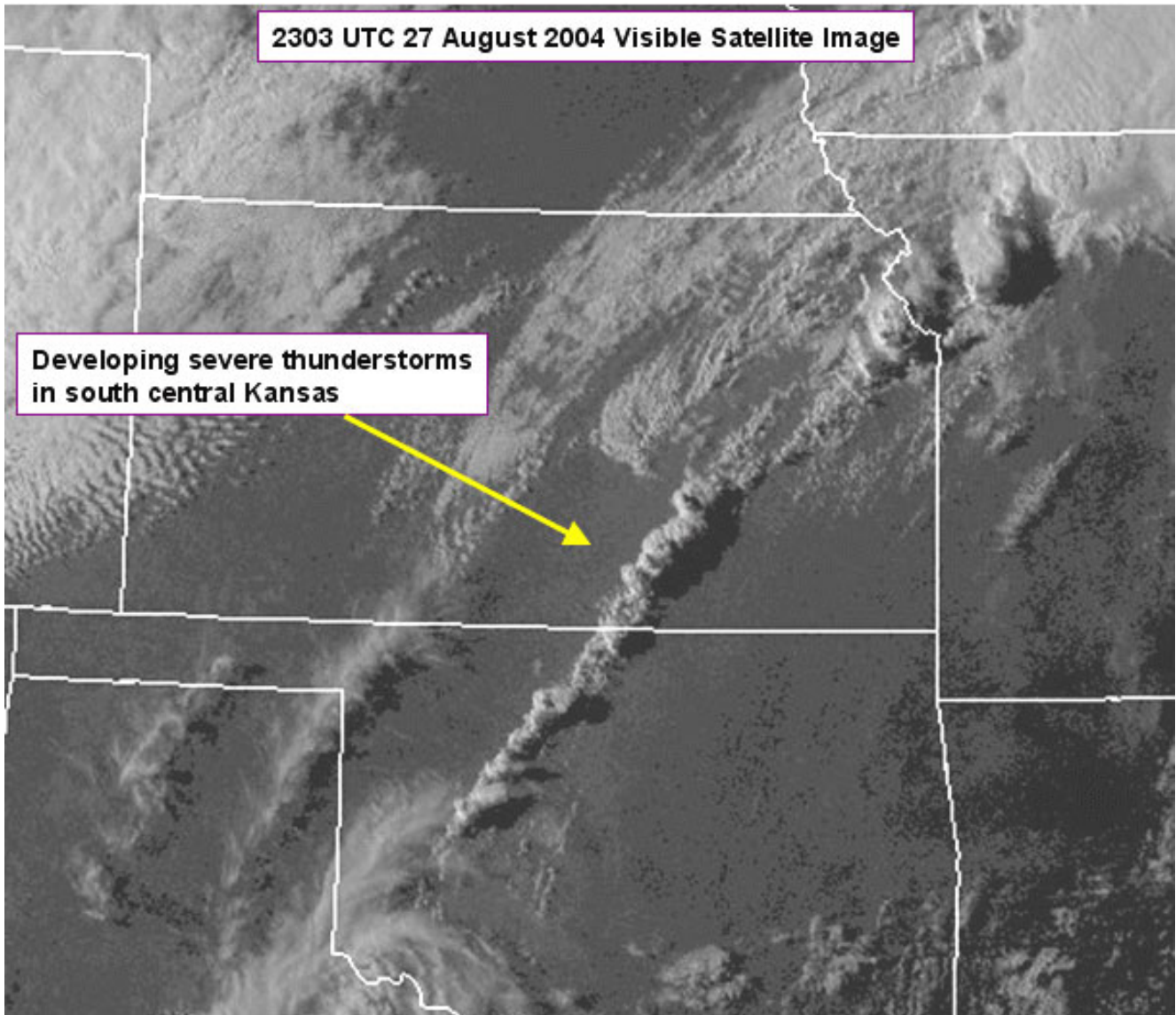


**Figure 8:** Visible satellite image at 2303 UTC 27 August 2004 depicting rapidly developing severe thunderstorms across south central Kansas. Image ©2004 UCAR <http://www.rap.ucar.edu/weather/satellite/>

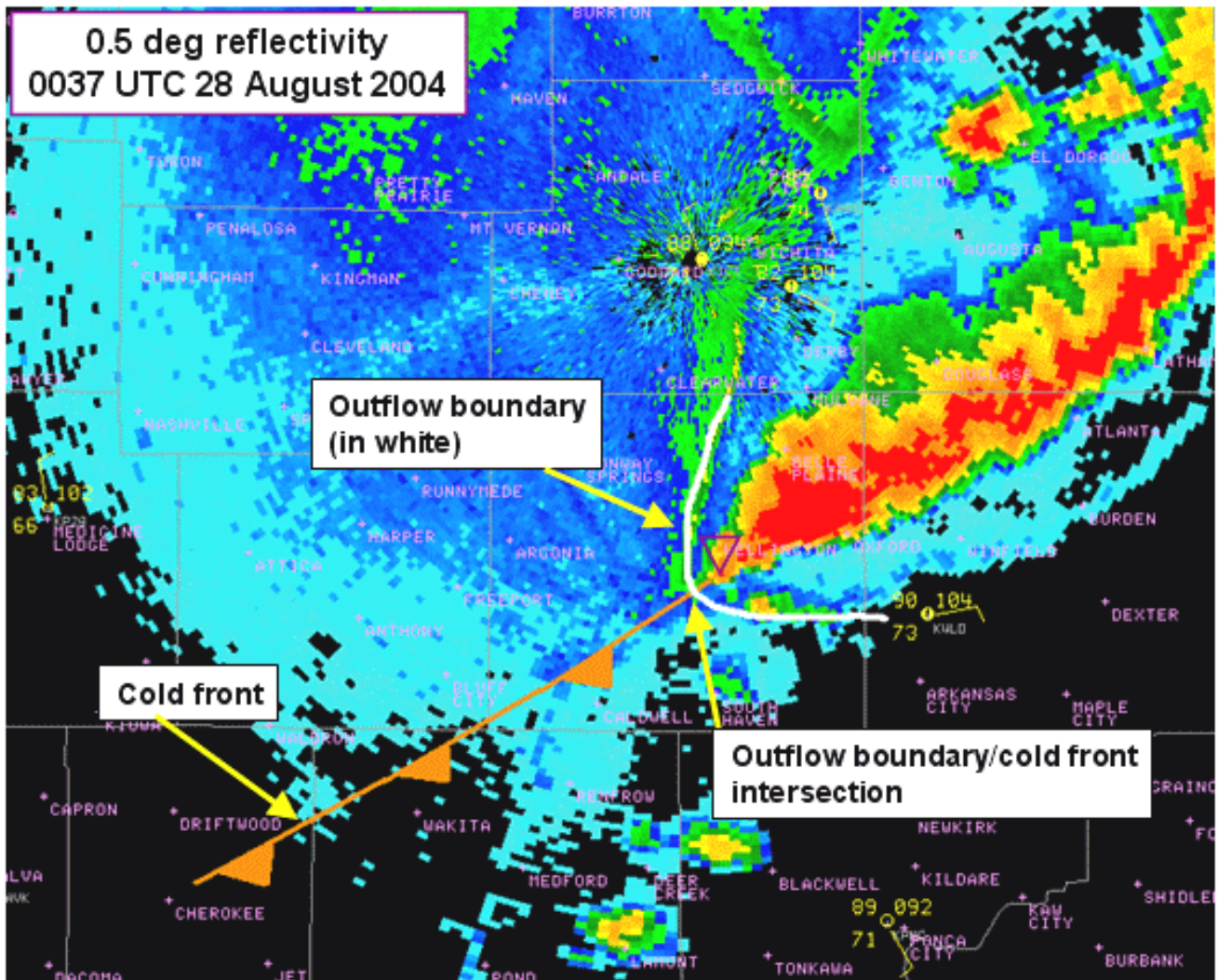


**Figure 9a:** Radar base reflectivity image from KICT WSR-88D (0.5 degree elevation) at 0037 UTC 28 August 2004. Surface boundaries are superimposed and labeled. Purple triangle shows location of F2 tornado near Wellington, Kansas at the time of this image, approximately 175°/48 km (26 nm) from the KICT WSR-88D.

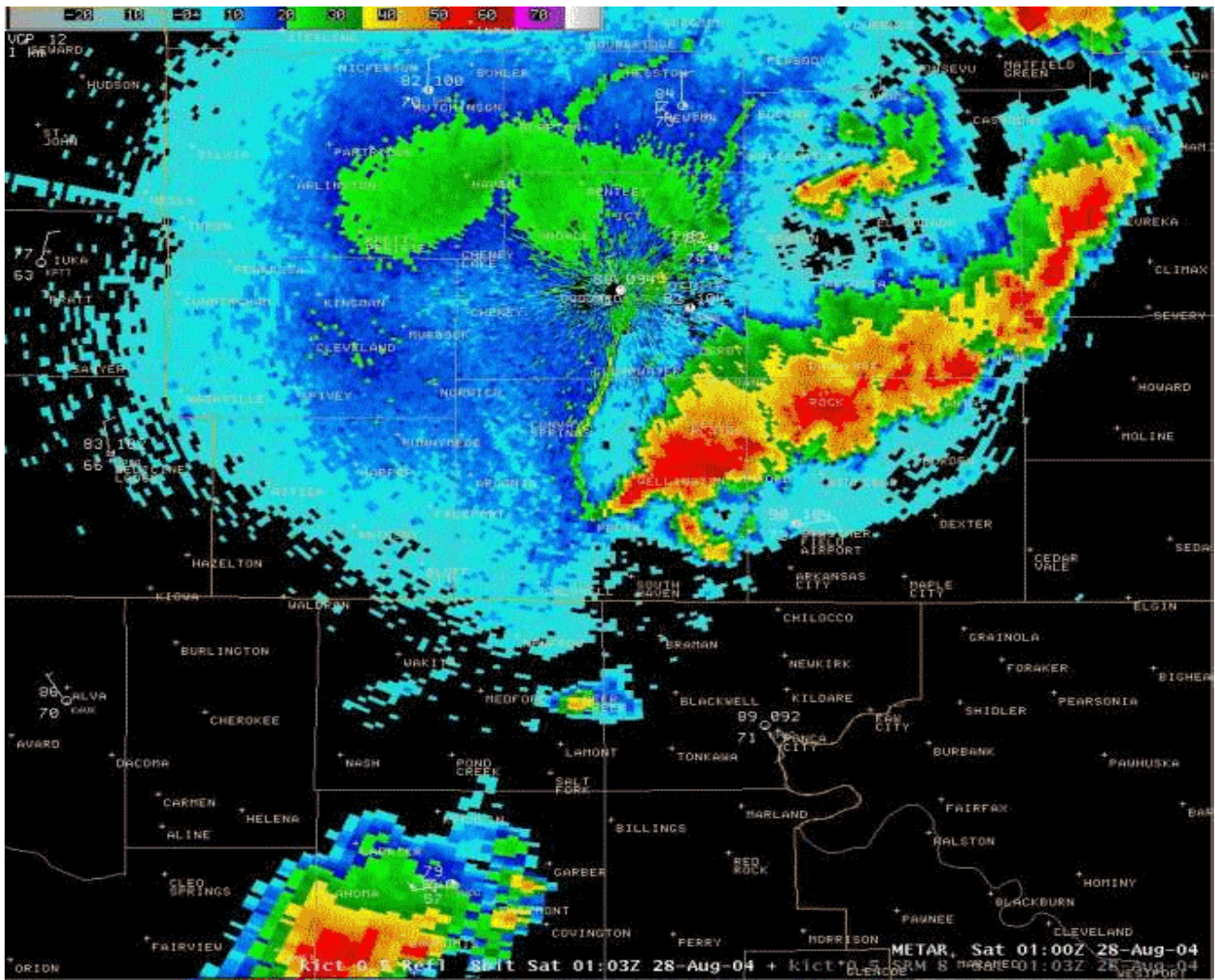


**Figure 9b:** Image loop from the KICT WSR-88D showing the 0.5 degree base reflectivity beginning at 2354 UTC 27 August 2004 and ending at 0103 UTC 28 August 2004. The individual images are in 9 minute increments. The F2 tornado was in progress from 0030 to 0049 UTC at the south end of the back-building storm cluster near the center of the image.

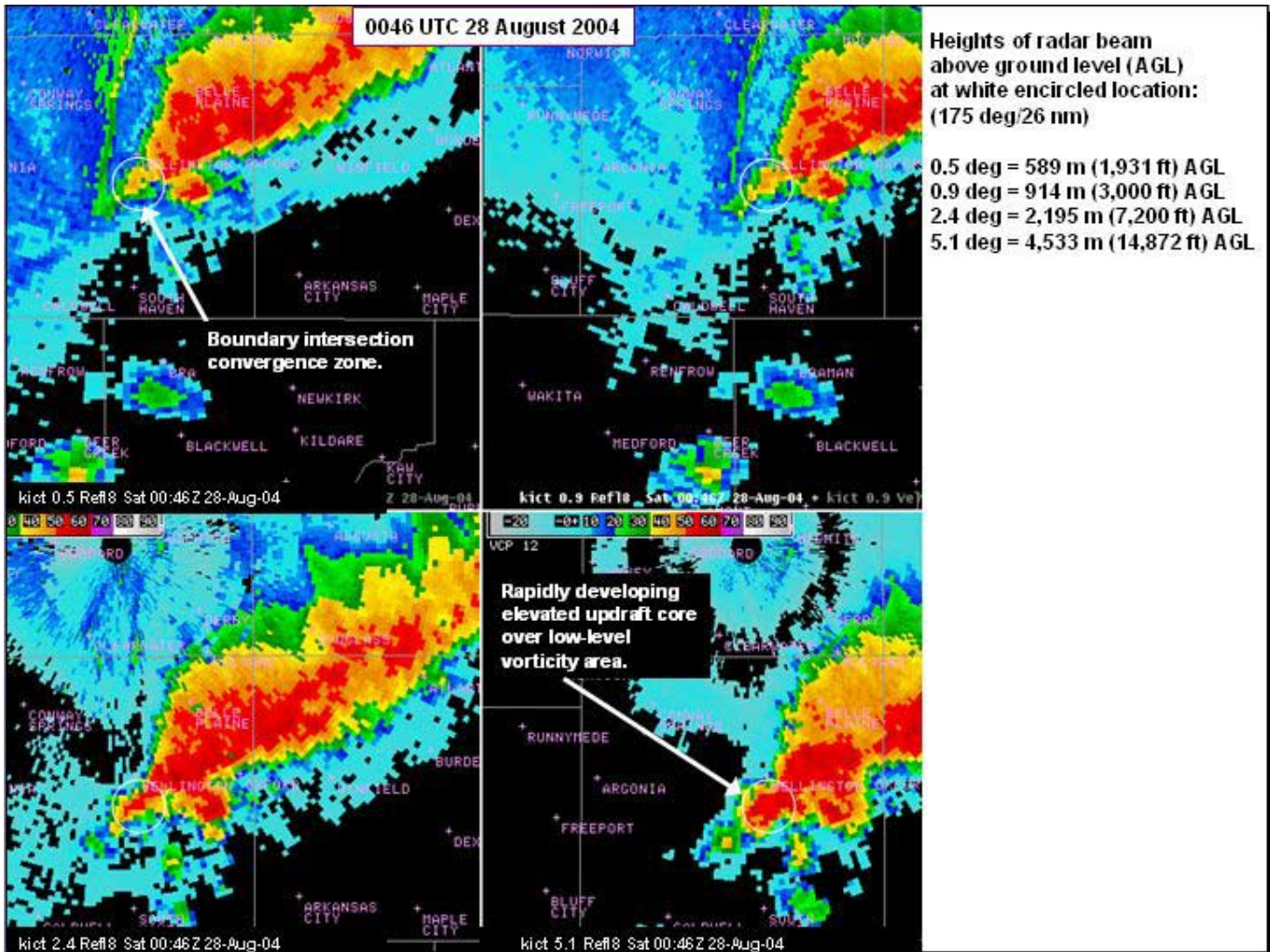


**Figure 10:** Radar base reflectivity 4-panel image from KICT WSR-88D at 0046 UTC 28 August 2004, showing elevation slices from 0.5 degrees to 5.1 degrees as labeled. White circles highlight area of interest where F2 tornado was occurring at intersection of frontal boundary and outflow.

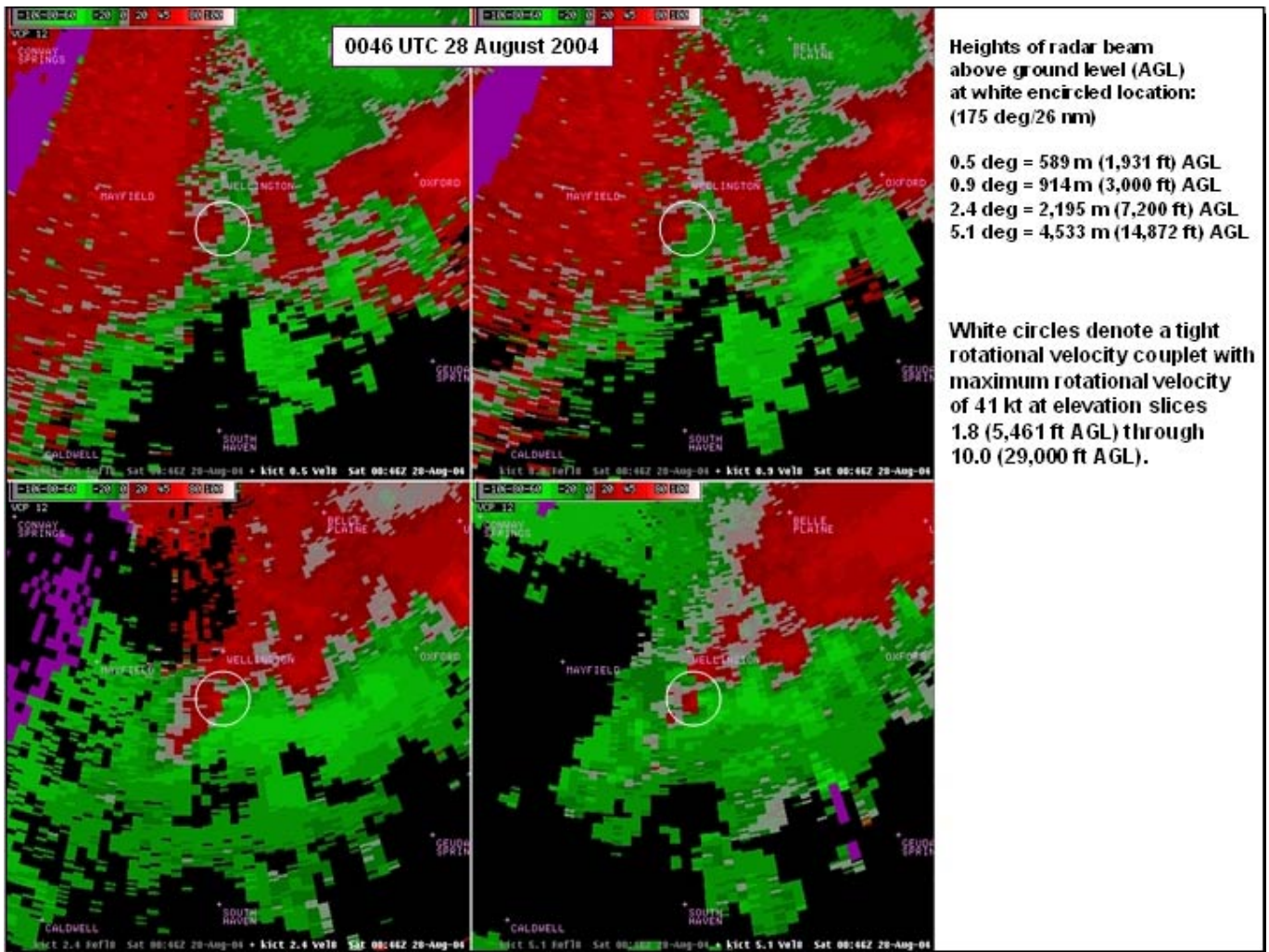
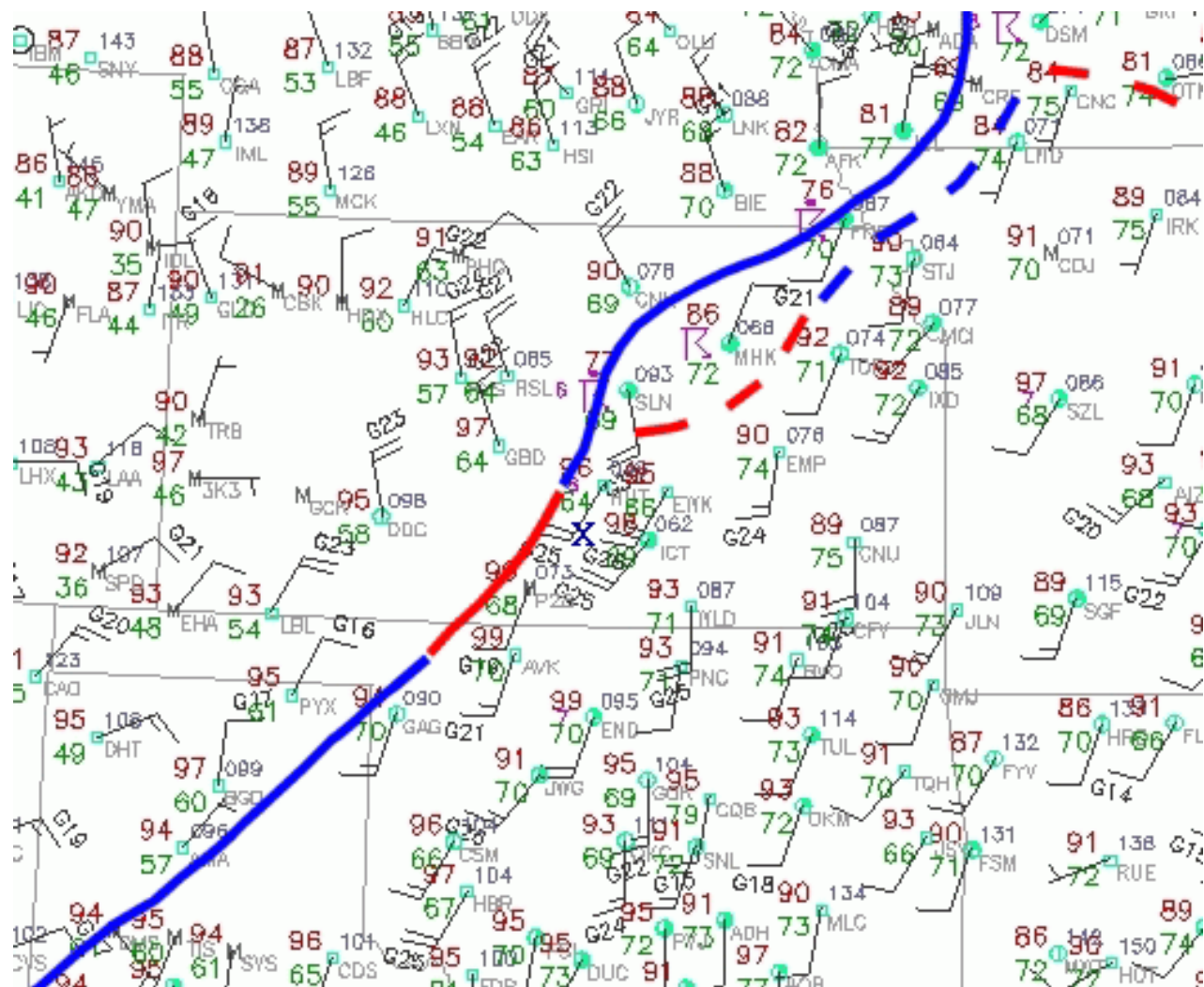
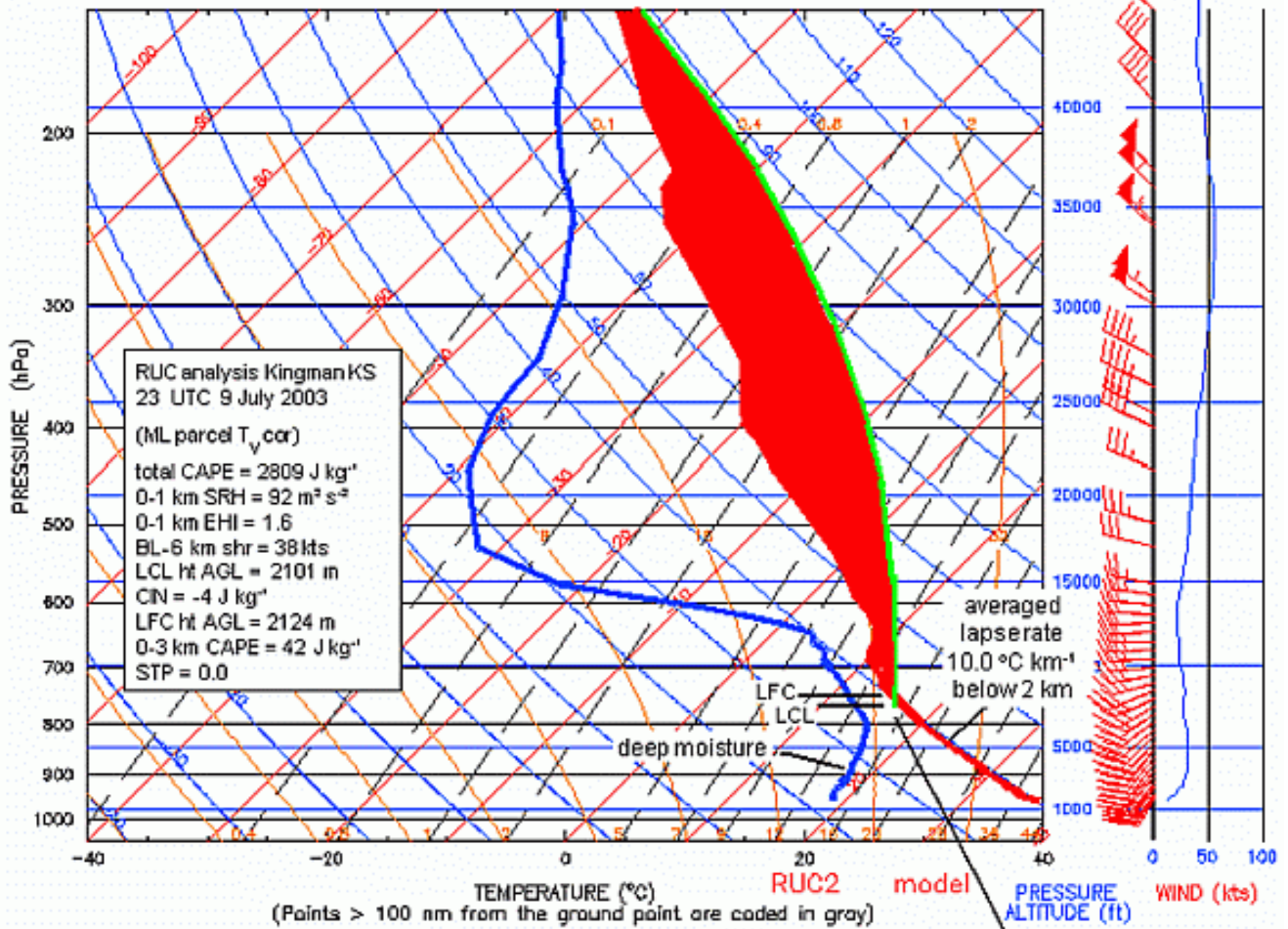


Figure 11: As in Fig. 10, except 4-panel image of base velocity for same time and elevation slices.



**Figure 12:** Surface map at 2300 UTC 9 July 2003 with frontal (solid) and outflow (dashed) boundaries indicated. The letter "X" denotes the location of the RUC model analysis sounding shown in Fig. 13.

RUC2 sounding for (-98.14, 37.48)  
23 UTC, 9-Jul-2003



Sounding from the RUC2 analysis

**Figure 13:** SkewT-logp diagram of RUC analysis sounding for Kingman, Kansas at 2300 UTC 9 July 2003, location shown in Fig. 12. Important features are labeled.

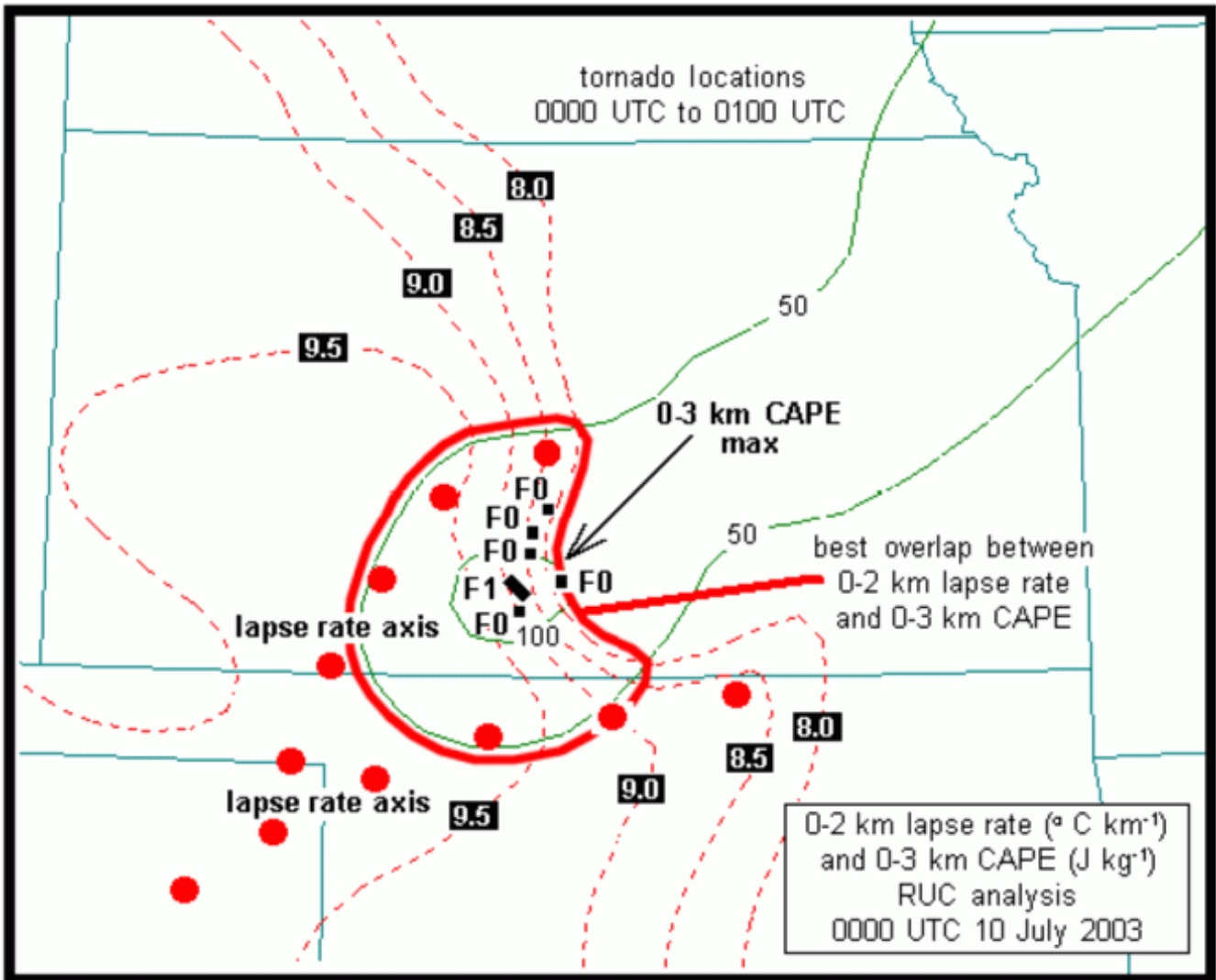


**Figure 14:** Overlapping fields of 0-2 km lapse rate and 0-3 km CAPE as in Fig. 7, except at 0000 UTC 10 July 2003. Tornado path locations 0000 UTC to 0100 UTC are shown in black with F-scales.

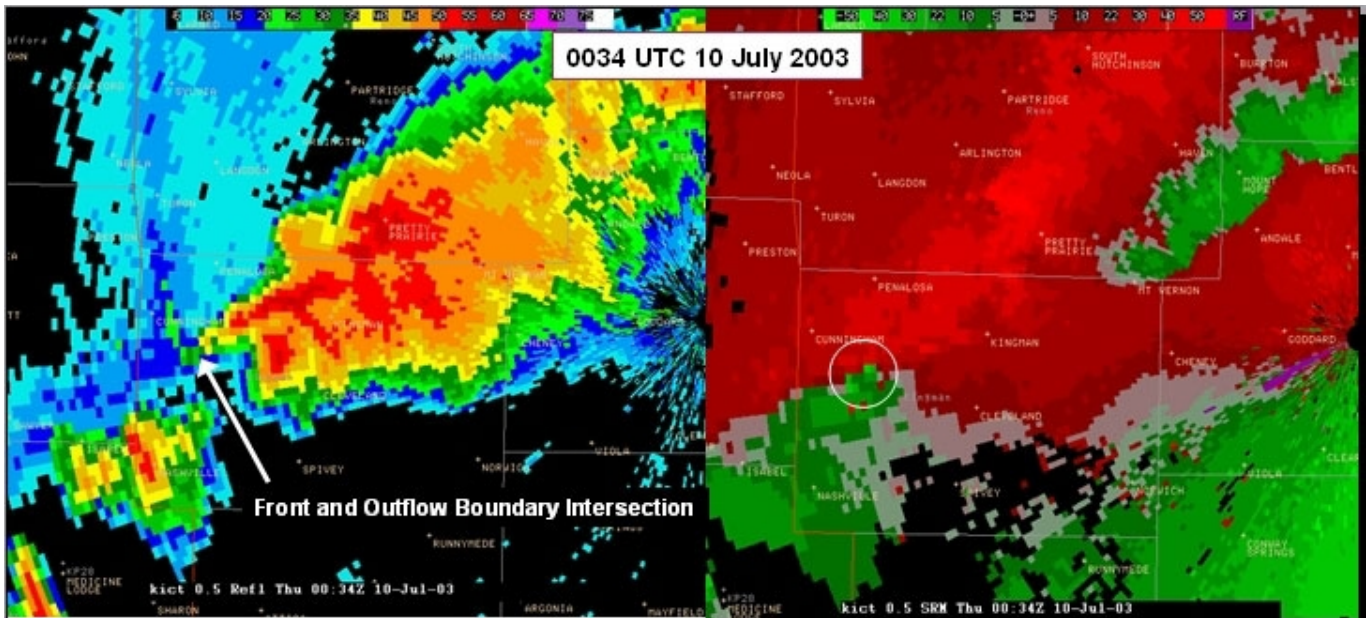


**Figure 15a:** Radar images showing KICT WSR-88D base reflectivity (left side) and storm-relative velocity (right side) at 0.5 degree elevation at 0034 UTC 10 July 2003. An important boundary intersection is labeled in the left image; the white circle in the right image indicates two weak rotational velocity couplets southeast of Cunningham, Kansas, located about 266°/82 km (44 nm) from the KICT WSR-88D, near the location of the F1 tornado in progress at the time of this image.

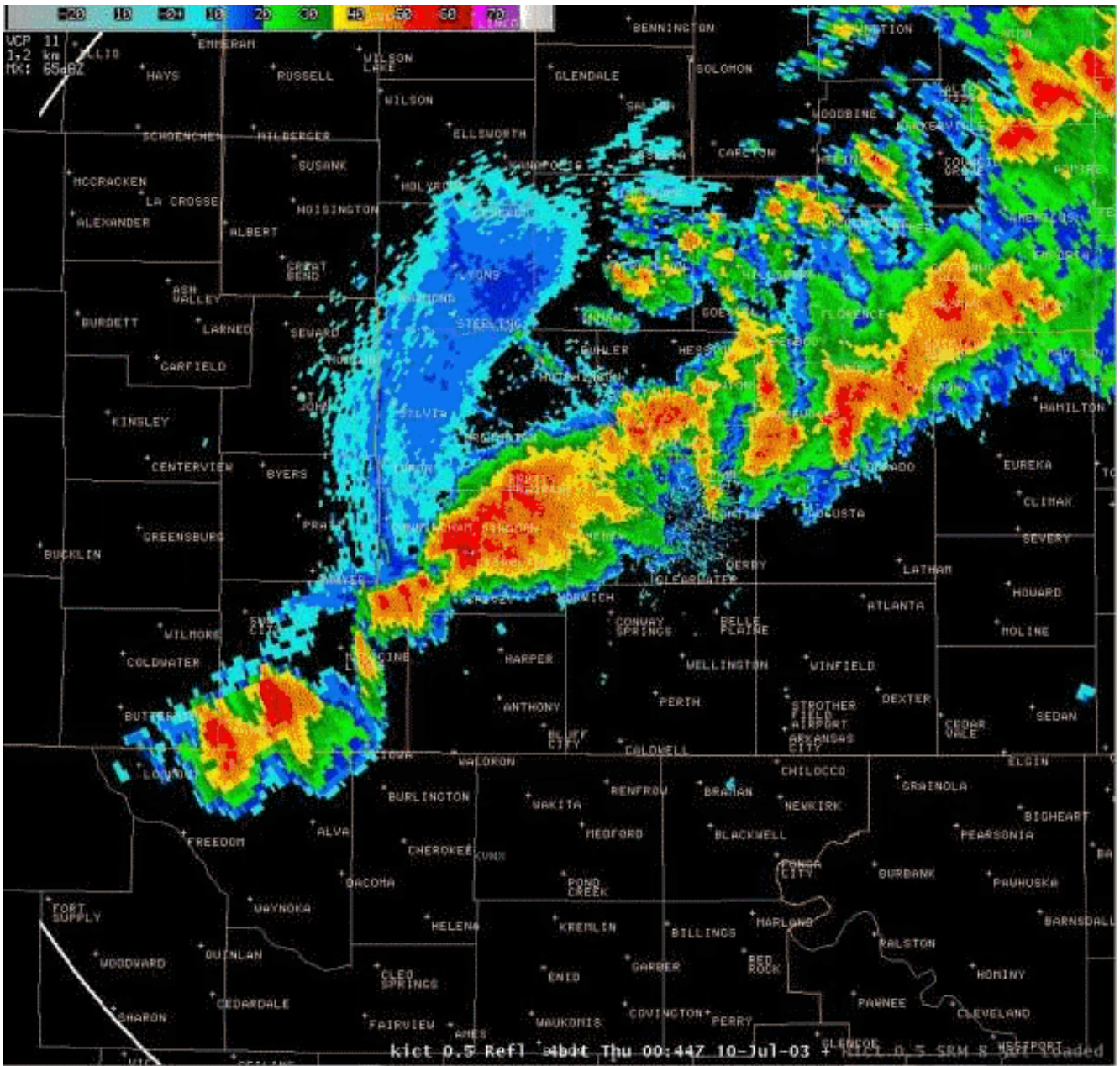


**Figure 15b:** Image loop from the KICT WSR-88D showing the 0.5 degree base reflectivity beginning at 2324 UTC 9 July 2003 and ending at 0044 UTC 10 July 2003. The individual images are in 10 minute increments. Tornadoes occurred intermittently from 2320 to 0109 UTC with the back-building storm and southward-moving boundary intersection near the center of the image.



**Figure 16:** Nonmesocyclone tornado southeast of Pretty Prairie, Kansas on April 11, 2002 (video images courtesy Jim Reed Photography <http://www.jimreedphoto.com/>)

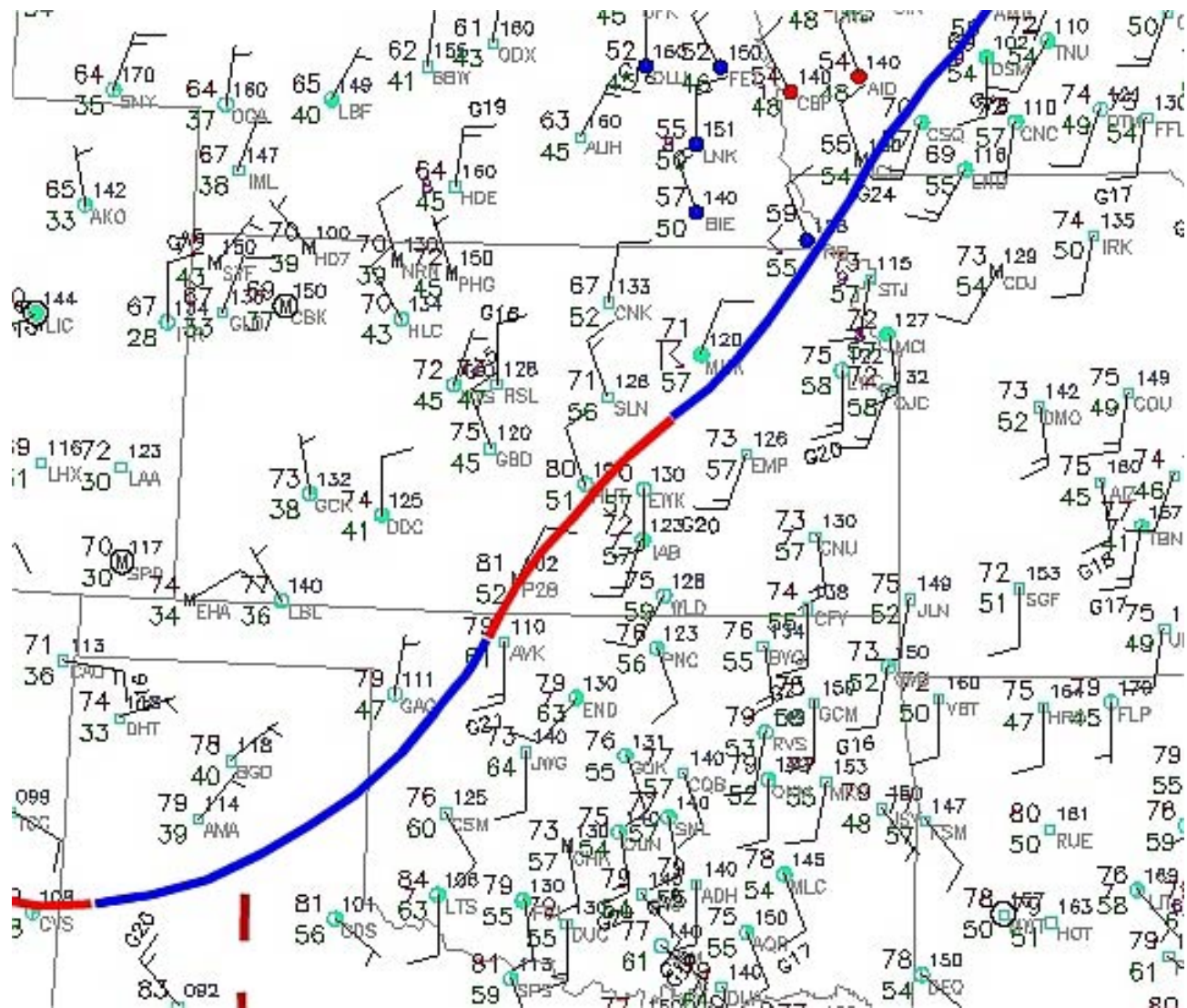
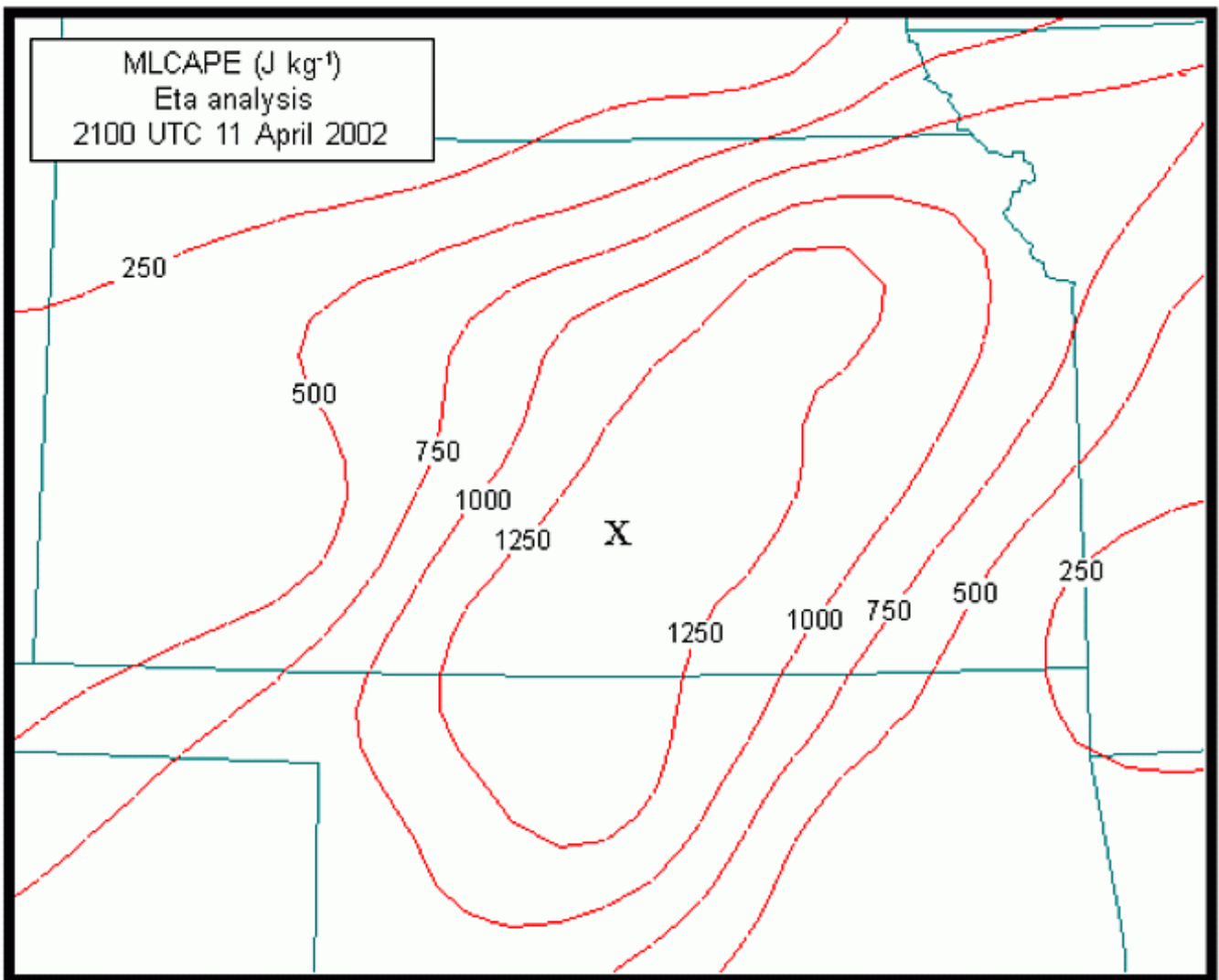


Figure 17: Surface map at 2300 UTC 11 April 2002, with frontal boundary indicated.



**Figure 18:** Estimated field of MLCAPE ( $\text{J kg}^{-1}$ ) computed from Eta analysis at 2100 UTC 11 April 2002. The letter "X" denotes the location of the RUC model analysis sounding shown in [Fig. 19](#).

RUC2 sounding for Hutchinson, KS/US  
22 UTC, 11-Apr-2002

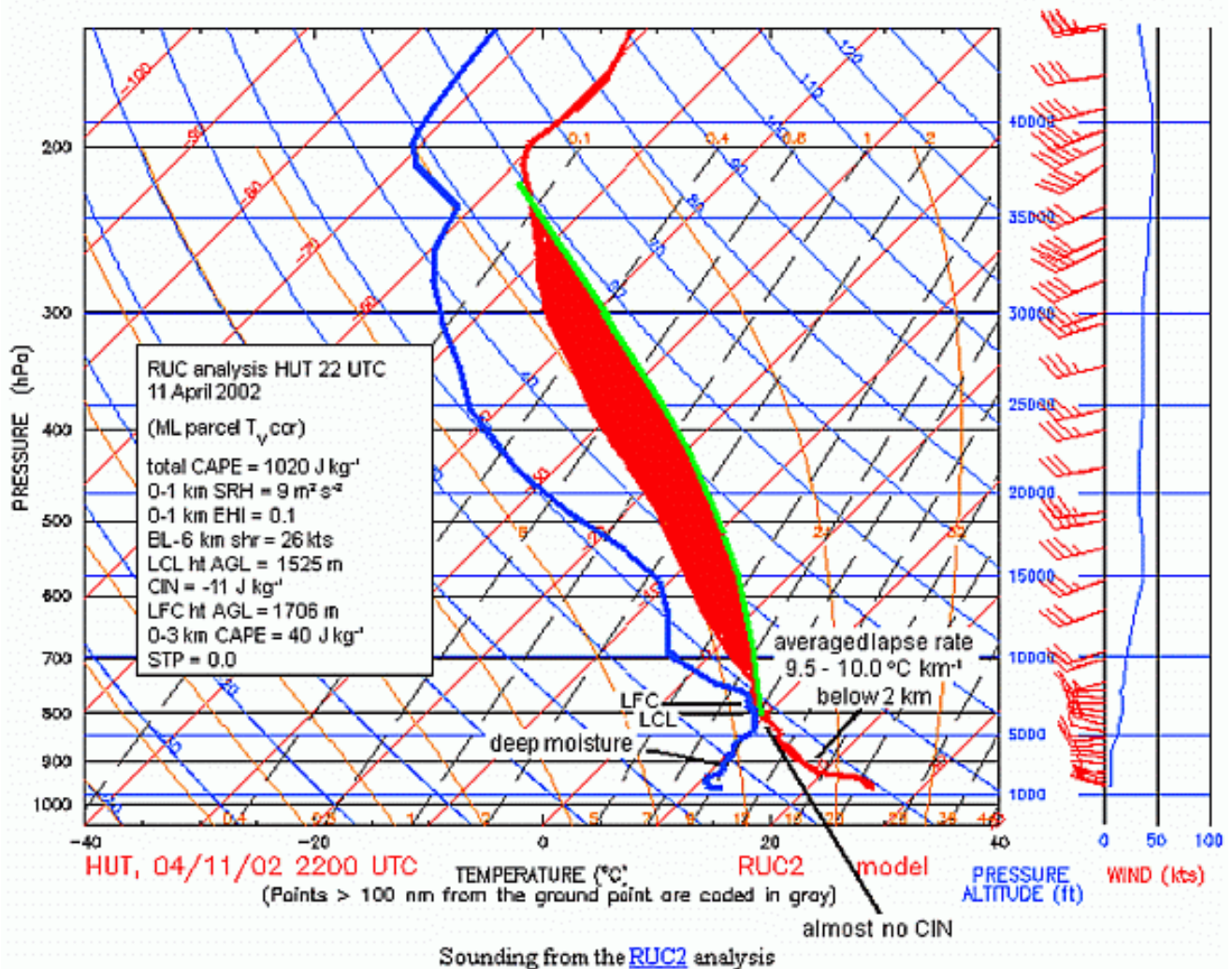
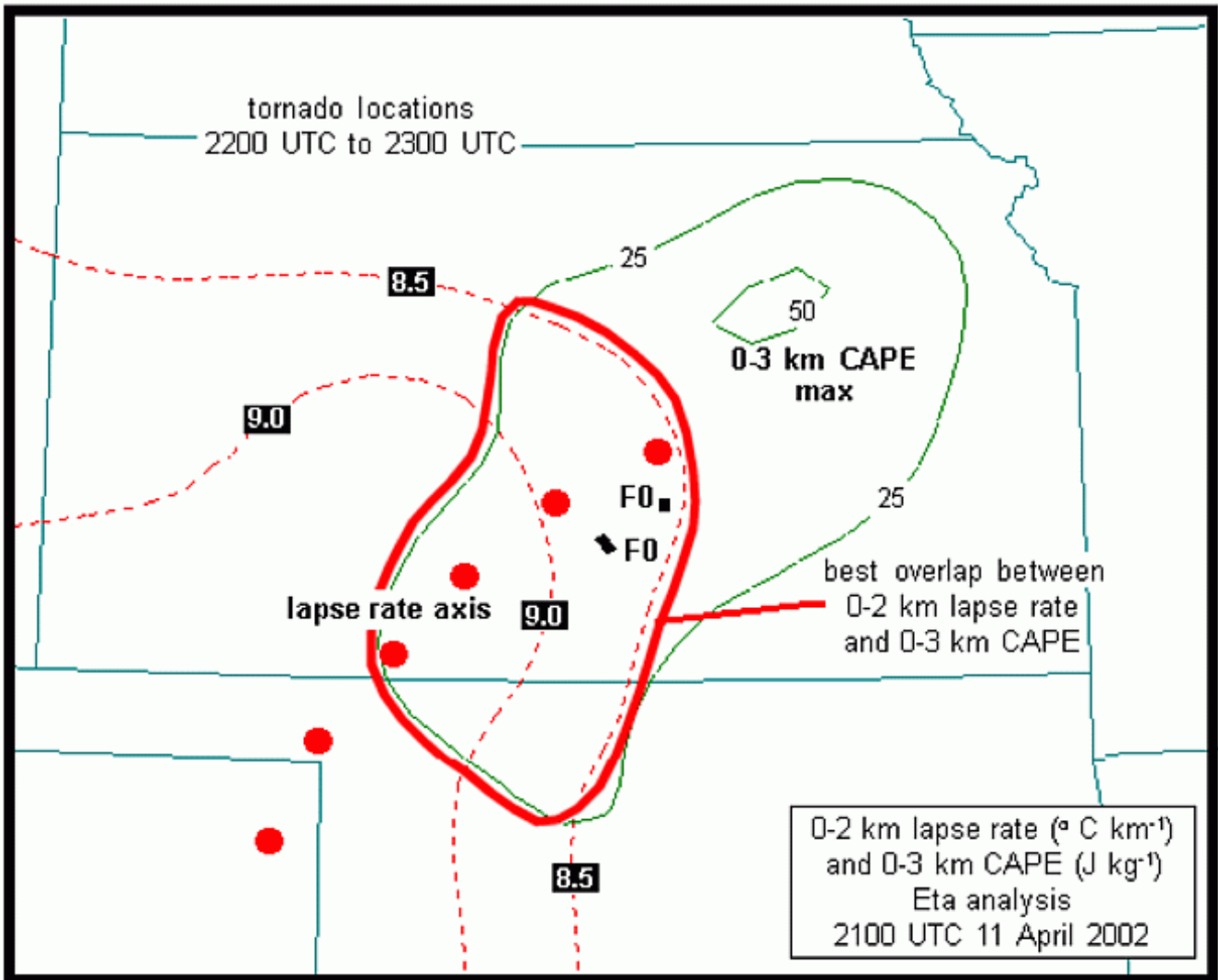
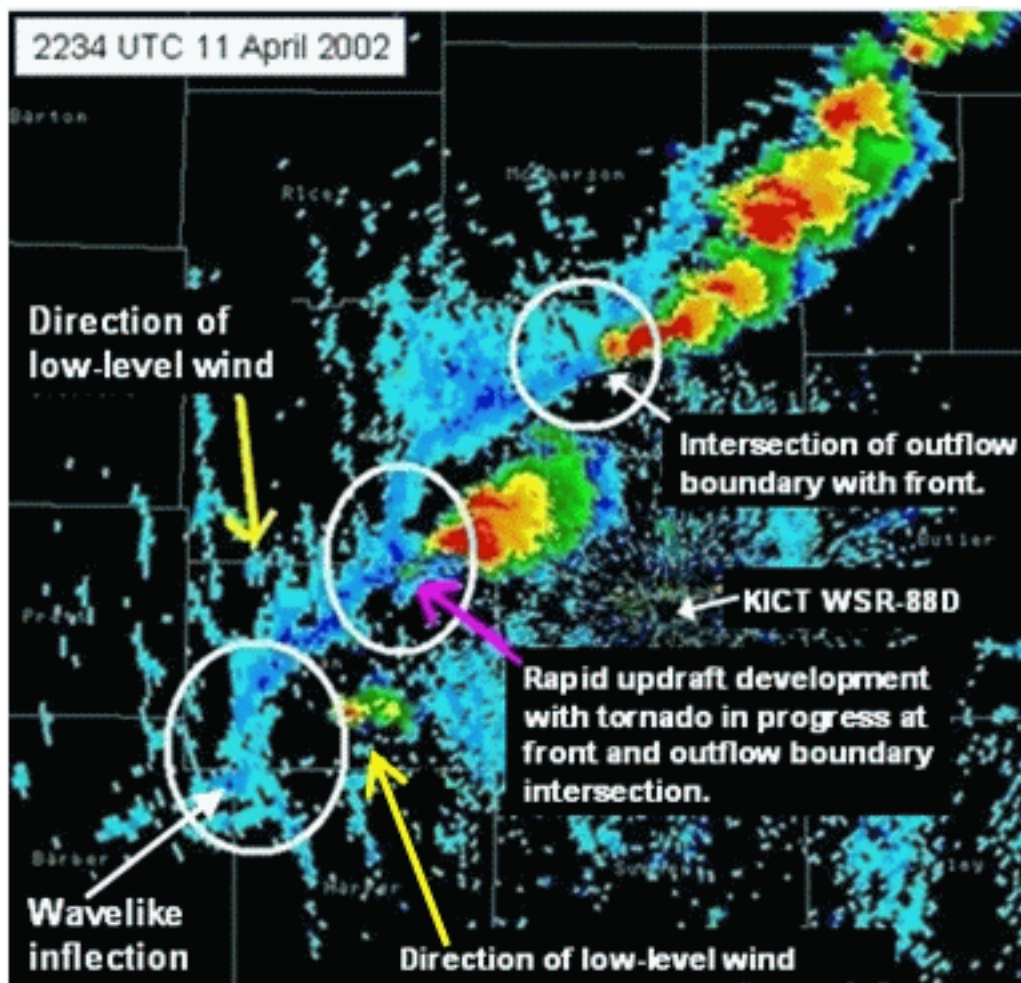


Figure 19: SkewT-logp diagram of RUC2 analysis sounding for Hutchinson, Kansas at 2200 UTC 11 April 2002, location shown in Fig. 18. Important features are labeled.



**Figure 20:** As in Fig. 18, except for 0-2 km lapse rate and 0-3 km CAPE from Eta analysis at 2100 UTC 11 April 2002, conventions similar to Fig. 7 and Fig. 14. Tornado path locations 2200 UTC to 2300 UTC are shown in black with F-scales.



**Figure 21a:** Radar base reflectivity image from KICT WSR-88D (0.5 degree elevation) at 2234 UTC 11 April 2002 with important features labeled. Yellow arrows depict direction of low-level wind flow; white ellipses indicate likely areas of pre-existing vertical vorticity; purple arrow points to location of new updraft developing at intersection of frontal boundary and outflow where a tornado was in progress. The tornado occurred approximately 285°/52 km (28 nm) from the KICT WSR-88D.

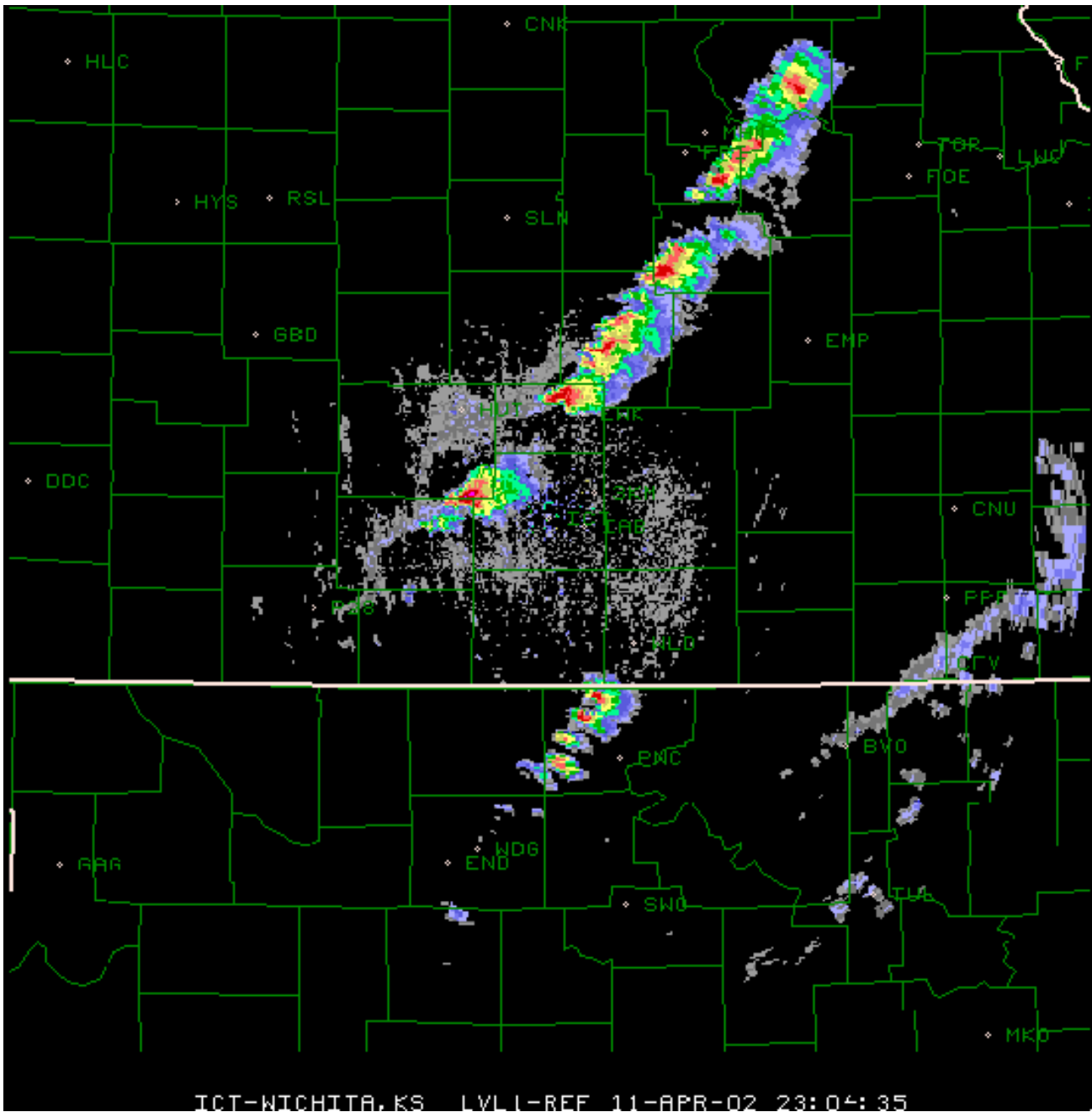


**Figure 21b:** Image loop from the KICT WSR-88D showing the 0.5 degree base reflectivity beginning at 2204 UTC 11 April 2002 and ending at 2309 UTC 11 April 2002. The individual images are in 10 minute increments. The tornado discussed in the text occurred from 2219 UTC to 2235 UTC with the southern-most, back-building storm near the center of the image.